Adaptive Optics Ophthalmoscopy

Austin Roorda[1] and Jacque L. Duncan[2]

[1]School of Optometry, University of California, Berkeley, Berkeley CA 94720; email: aroorda@berkeley.edu

[2]Department of Ophthalmology, University of California, San Francisco, San Francisco, CA 94143

Keywords

adaptive optics, ophthalmoscopy, retina, scanning laser ophthalmoscopy, fundus camera

Abstract

This review starts with a brief history and description of adaptive optics (AO) technology, followed by a showcase of the latest capabilities of AO systems for imaging the human retina and by an extensive review of the literature on clinical uses of AO. It then concludes with a discussion on future directions and guidance on usage and interpretation of images from AO systems for the eye.

1. INTRODUCTION

AO: adaptive optics

OCT: optical coherence tomography

SHWS: Shack–Hartmann wavefront sensor

The use of adaptive optics (AO) converts an ophthalmoscope into a microscope, allowing visualization of and optical access to individual retinal cells in living human eyes in ways not previously possible (Liang et al. 1997). This microscopic access is driving a paradigm shift in how we use ophthalmoscopy to study vision and visual dysfunction.

AO is a technology that was originally developed by astronomers to sharpen images by compensating for the blur-inducing optical aberrations caused by turbulence within the atmosphere of the Earth. In the field of vision science, AO compensates for optical aberrations in the optics of the eye and can be applied to any ophthalmoscope modality, including full-field fundus cameras, scanning laser ophthalmoscopes (SLOs), and optical coherence tomography (OCT) systems. This review concerns only the first two modalities, as they have yielded the majority of clinical research published to date. In addition, OCT has had such a profound impact in the field of ophthalmology that it warrants its own dedicated review.

AO technology for ophthalmoscopy is relatively young, and new technical developments; new applications; and new approaches to the analysis, interpretation, and presentation of results are appearing monthly. Considering this, the review places as much emphasis on emerging applications of AO technology that are relevant for clinical ophthalmic applications (Section 3) as on what has already been learned (Section 4). The aim is to offer guidance on exciting new clinical directions that AO users and developers should consider. Another aim is to point out some areas of AO research, specifically those related to image analysis and interpretation, that beg for more attention (Section 5).

# 2. WHAT IS ADAPTIVE OPTICS?

An AO system involves two important steps: measuring the optical imperfections of the eye and compensating for them. This compensation is generally done over the largest pupil size possible to maximize the numerical aperture (see the sidebar What Is the Difference Between a Microscope and an Ophthalmoscope?).

Aberrations in the eye can be measured in several ways, but the Shack–Hartmann Wavefront Sensor (SHWS), which made AO possible, seems, by all accounts, to be the best available approach to measure aberrations in the human eye. Junzhong Liang was the first to develop a SHWS for the human eye as part of his PhD research for Heidelberg University with Josef Bille (Liang et al. 1994), and the SHWS was further refined at the University of Rochester (Liang & Williams 1997).

Recognizing the enabling potential of SHWS technology for ophthalmic applications, Junzhong Liang and Donald Miller, led by David Williams, built the world's first AO retinal camera (Liang et al. 1997). The key technology was a deformable mirror that could be shaped in such a way as to give it an aberration equal and opposite to that of the eye, as measured by the SHWS. Thus, the aberrations in the beam of light emerging from the eye effectively would be cancelled by the aberrations of the mirror. For more details on AO technology, the reader is referred to the following texts (Miller & Roorda 2009, Porter 2006, Roorda 2011, Williams 2011). The benefits of using AO for ophthalmoscopy were realized immediately, as the images from the first AO fundus camera were the first to show resolved arrays of human cone photoreceptors (Liang et al. 1997).

It is no coincidence that the fundus camera was the first ophthalmic imaging modality adopted for AO. Fundus cameras employ simple optical principles and involve little more than a camera forming an image on a light-sensitive film (or CCD) of the light emerging from the retina through the optics of the eye. Thus, implementing AO is only a matter of placing the corrector at an appropriate location between the camera and the eye. In fact, any ophthalmic device that involves

WHAT IS THE DIFFERENCE BETWEEN A MICROSCOPE AND AN OPHTHALMOSCOPE?
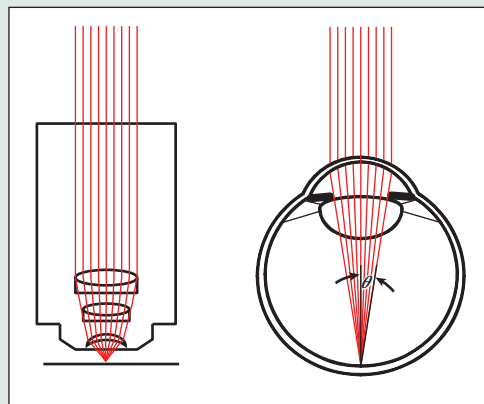
Microscopes and ophthalmoscopes are essentially the same, except that in an ophthalmoscope, the optics of the eye always serve as the objective lens, and the sample is always the retina or some other part(s) of the ocular fundus. The same rules govern the image quality in both. Specifically, the numerical aperture (*NA*) is given by the following equation:

$$NA = n \cdot \sin(\theta) = n \cdot \sin\left(\arctan\left(\frac{D}{2 \cdot f}\right)\right),$$

where *n* is the index of refraction of the media in which the light is focused, θ is the half angle of the focused beam at the sample, *D* is the entrance pupil diameter (beam size), and *f* is the focal length. For a human eye, *NA* ranges from 0.03 to 0.2 (for a 1–7-mm pupil). In contrast, microscope optics can be designed with very steep focusing angles and *NA* values that are greater than 1. The resolution *R* (the smallest resolvable distance between two point objects) is related to the *NA* and often quantified with the following equation:

$$R = \frac{\lambda}{2 \cdot NA},$$

where λ is the wavelength of the light passing through the system.

An ophthalmoscope can potentially resolve features as small as 1.3 μm (using a 7-mm beam and 550-nm light), whereas a microscope with an *NA* of 1 can resolve 0.275 μm. However, the equation for *R* applies to only diffraction-limited systems (those for which the only limit to resolution is the diffraction of light). Aberrations in the eye make the resolving power of an ophthalmoscope much worse; thus, adaptive optics are needed.

passing light into or out of the eye could benefit from AO. The benefit is limited not only to ophthalmoscopes, but also to vision testing systems (Fernández et al. 2009, Guo et al. 2008, Roorda 2011, Sawides et al. 2010, Schwarz et al. 2014, Yoon & Williams 2002). One ophthalmic imaging technology that is particularly well-suited for AO is the scanning laser (or light) ophthalmoscope (SLO). Invented in 1980 by Robert Webb (Webb et al. 1980), the SLO forms an image over time by continually recording and logging the light scattered from a single focused spot on the retina as it is scanned across the retina, generally in a raster pattern. Because they are able to record movies of the retina at video rates, SLOs can be used in a vast number of ways. The most common mode of imaging is confocal imaging, which uses a small aperture (confocal pinhole) positioned close to the detector and optically conjugate to the focused spot on the retina. The confocal pinhole blocks scattered light from reaching the detector, with the exception of light arriving from near the plane of focus. The use of this confocal pinhole thereby enables optical sectioning, which is the primary advantage of confocal microscopes over conventional light-field microscopes. In the human eye, the confocal pinhole allows for some optical sectioning (although this ability is not close to the axial sectioning ability of OCT), but it also provides high-contrast images of the structure of interest.

The first application of AO to an SLO was reported by Roorda et al. (2002). That paper demonstrated the video-rate imaging and confocal advantages of the SLO in the measurement of blood cell velocity and rudimentary optical sectioning. The complexity of the design and the

reliance on partially coherent light sources (Putnam et al. 2010) were limiting factors in using SLOs early on, but these limitations have mostly been overcome as a result of innovative optical design (Dubra & Sulai 2011) and the availability of better light sources (Zhang et al. 2006). Today, AOSLOs in research labs are producing en face retinal images with higher contrast and resolution than any other imaging modality. In fact, the best AOSLOs appear to have achieved a resolution that is effectively at the diffraction-limit for eyes with clear optical media (Dubra et al. 2011).

The implementation of AO in an ophthalmoscope is only the first step in realizing its full range of benefits. Consider, for comparison, the field of microscopy. Today, the use of a microscope to look at scattered or transmitted light from biological specimens represents only one of many possible applications. Almost every modern use of the microscope employs contrast agents, fluorescent labels, or innovative illumination and detection schemes, and the arsenal of tools available to the microscopist is expanding. Although standard approaches that involve recording scattered light from the retina have proven useful for both fundus camera and SLO modalities, the reflected or scattered light does not provide specific information about the function or health of a retinal cell. Even the simple notions that a visible cone is healthy or that an invisible cone indicates visual dysfunction have been questioned (Wang et al. 2015). However, this review describes the expanding array of more innovative uses of AO technology within these modalities, and it argues that we have witnessed only the very beginning of what can be done. Put simply, AO offers microscopic optical access, and the ophthalmoscopist must determine how to employ that access.

3. STATE OF THE ART IN ADAPTIVE OPTICS IMAGING TECHNOLOGY

This section showcases the capabilities of current AO systems and is intended to show that AO is still a developing technology. Had we focused solely on clinical applications, this review would have failed to give the reader an appreciation of the potential capabilities of AO, as actual clinical studies can be complicated with an emerging technology. The time with a patient is limited; the patients and the operators are often less familiar with the technology than are those who build it; and many patients may not have optimal fixation, lens clarity, tear film stability, or patience, all of which can compromise the quality of the data collection. Nevertheless, AO is already having an impact in ophthalmology as shown in Section 4.

3.1. Imaging Structure

Visualizing microscopic structure in the retina requires a combination of resolution, contrast, and a sufficient signal-to-noise ratio (SNR) (for definitions of these terms, see the sidebar Image Quality Metrics). AO offers sufficient resolution in all cases, but sufficient contrast and SNR can be reached in many different ways. In this section, we showcase the best images of all the retinal structures imaged to date in healthy eyes using all the current AO imaging modalities, with the exception of AO-OCT. Most imaging modalities included here have been used on humans, but we have added insets to figures taken from animals to indicate the species when applicable.

3.1.1. Nerve fiber layer. Axons of the ganglion cells traverse across the surface of the retina, forming the nerve fiber layer (NFL). The NFL is a relatively strong source of backscatter, and its microstructure has been resolved with confocal AOSLO imaging (Huang et al. 2014, Takayama et al. 2012) and AO fundus cameras (Ramaswamy et al. 2014). **Figure 1** shows a confocal AOSLO image of discrete, individual, nerve fiber bundles originating from the temporal raphe. This region

IMAGE QUALITY METRICS

Image quality can be defined using three metrics: resolution, contrast, and the signal-to-noise ratio (SNR).

Resolution is the ability of an imaging system to allow two adjacent structures to be visualized as being separate or the distinctness of an edge in the image (i.e., its sharpness).

Contrast is the difference in luminance and/or color that makes an object (or its representation in an image or display) distinguishable.

The SNR is the ratio of the power between the signal strength and the background noise.

The following images of a letter E against a background illustrate the differences.

Limited by blur	Limited by contrast	Limited by noise

Although these qualities can be considered independently, they are related. For example, improved resolution (offered by AO) improves the contrast of higher frequencies, thereby increasing the overall contrast and SNR. But, an image of a low-contrast and/or low-SNR object with low contrast may never be visualized, no matter how high the resolution.
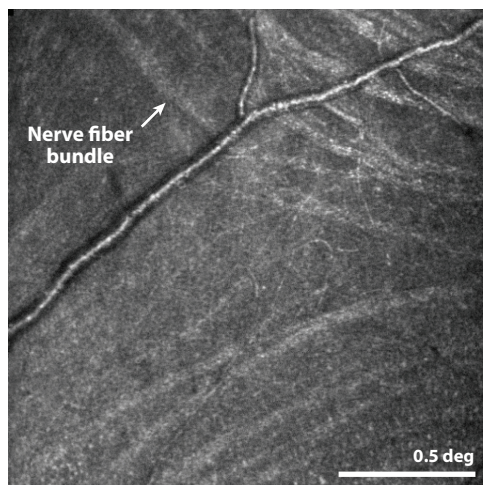

Figure 1

This confocal adaptive optics scanning laser ophthalmoscope (AOSLO) image shows the location at which nerve fiber bundles originate, temporal to the fovea (not shown, but located to left of the image). The line separating bundles that traverse above and below the fovea is the called the temporal raphe. In the original paper, the authors carefully map its location relative to the fovea and optic disk and show individual variability and changes with age. Figure adapted with permission from Huang et al. (2014).
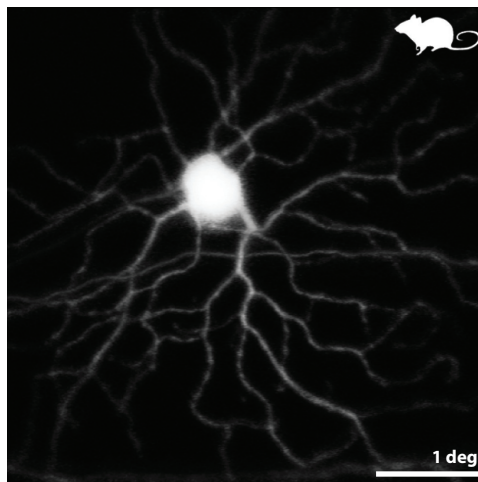
Figure 2

Fluorescence adaptive optics scanning laser ophthalmoscope (AOSLO) image of the retina of a living mouse expressing yellow fluorescent protein (YFP) in a fraction of its ganglion cells (GCs). This image shows a monostratified ON GC. ON or OFF types were identified by resolving—through confocal optical sectioning—the sublamina of the dendrites within the inner plexiform layer. Figure adapted with permission from Geng et al. (2012).

is vulnerable to vision loss in glaucoma, and closer examination of it will help provide both a better understanding of it and an ability to monitor changes in this structure.

3.1.2. Ganglion cells. Although the NFL is directly visible, the originating ganglion cells (GCs) have proven more elusive. Their relatively large size makes them resolvable, but they are weakly scattering (low SNR) and, in back-reflected light, do not seem to possess the intrinsic contrast that might reveal their structure. To date, visualization of the GCs in living eyes has only been possible using extrinsic fluorophores. Specially designed AOSLO systems in conjunction with extrinsic fluorophores of various types have been employed to visualize GCs in monkeys (GCaMP3) (Yin et al. 2014), rats [enhanced green fluorescent protein (eGFP)] (Geng et al. 2009), and mice [(GCaMP3) (Yin et al. 2013) and yellow fluorescent protein (YFP)-expressing GC-specific genetic strains (Geng et al. 2012)]. **Figure 2** shows an example of a GC imaged in a YFP-expressing mouse. The image is especially well resolved partly because the mouse has a higher numerical aperture then the human (see the sidebar What Is the Difference Between a Microscope and an Ophthalmoscope?), offering higher potential resolution (Geng et al. 2011). In fact, the GC image shown here approaches the resolution typically obtained for in vitro preparations of the same cell. Today, the use of fluorescent agents, other than sodium fluorescein, indocyanine green (ICG), and fluorescent-conjugated annexin V, is not permitted in humans. Nevertheless, the ability to image these cells in mice has a major potential clinical impact, as mice are the most common animal model for studying retinal disease.

3.1.3. Vasculature. A healthy vascular network is crucial to the health and function of the retina. The standard clinical method to visualize the vasculature in a living human retina is to boost its contrast by recording fluorescence emission from systemically injected sodium fluorescein or ICG. Backscattered light in confocal AOSLO and AO fundus cameras has been only moderately successful in visualizing the microvasculature (Martin & Roorda 2009, Popovic et al. 2011).
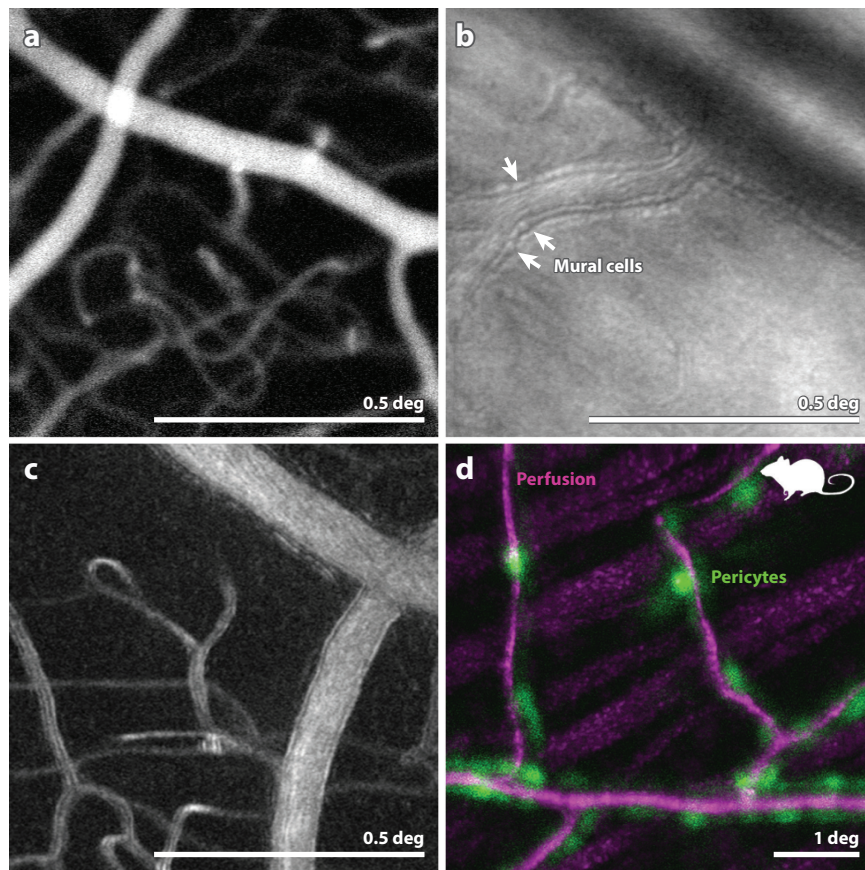
GC: ganglion cell

Figure 3

(*a*) Fluorescein angiography (FA) of a human retina with adaptive optics scanning laser ophthalmoscopy
(AOSLO). This particular implementation employed oral fluorescein, offering a longer time course for
imaging and avoiding risks associated with injection. The use of AOSLO offers higher contrast and higher
resolution over conventional FA. (*b*) Image of the microvascular structure of a human retina using offset-
pinhole AOSLO. Arrows point to purported individual mural cells that compose the arteriole walls. Panel
adapted with permission from Chui et al. (2013). (*c*) Motion contrast image from split-detector AOSLO
recordings of a vessel and capillary network in a normal human eye. Panel adapted with permission from
Sulai et al. (2014). (*d*) A combination of confocal AOSLO motion contrast of perfusion (*magenta*) and
fluorescent AOSLO images of tagged pericytes (*green*) in a mouse retina reveals the colocation of these
structures. Panel adapted with permission from Schallek et al. (2013).

Departures from conventional AO systems that detect backscattered light have proven to be
the most effective modalities for all aspects of vascular imaging. An obvious first example is the
combination of fluorescein angiography (FA) and AO. This combination takes advantage of the
high contrast of FA and the high resolution of AO and has yielded stunning images (Gray et al.
2006, Pinhas et al. 2013) (see **Figure 3***a*). But, although sodium fluorescein is very useful, FA is
invasive, generates its signal over a limited time course, and is not without side effects.

The biggest advances in vascular imaging have emerged through the use of nonconfocal
AOSLO detection schemes (large pinhole, offset pinhole, dark-field, and split-detector) and

through the use of motion contrast. These alternate detection schemes, which either block the direct backscattered component (split-detector or dark-field AOSLO) or are designed to admit more multiply-scattered light (offset pinhole), can extract more signal from the actual blood flow and more details of the microvascular structure. **Figure 3***b* shows an arteriole in which purported mural cells composing the vessel wall are visualized.

Another new source of contrast, motion contrast, emerged as a result of the ability to record AO-corrected videos of the retina. In a video of the retina, scatter from most features remains relatively constant, but scattering and shadowing from blood cells generate a dynamic signal. By processing the videos to highlight only the dynamic element of the signal, exquisite vascular maps have been generated. **Figure 3***c* shows one example of a motion contrast perfusion image extracted from an AOSLO video acquired with a split detector (Sulai et al. 2014). Incidentally, similar motion contrast approaches are also emerging in OCT angiography.

In microscopy, acquisition and cross-registration of images that encode different aspects of structure and function are effective tools for understanding complex systems (e.g., multiple fluorescent labels in microscopy), and similar benefits are beginning to be realized for retinal imaging. **Figure 3***d* shows a fluorescent image of pericytes overlayed onto a motion contrast image of the retinal vasculature.

3.1.4. Bipolar cells. To date, no AO system has reported on the visualization of bipolar cells. Similar to GCs, bipolar cells are resolvable but lack the scatter and intrinsic contrast to be readily seen by reflectance. Thus, fluorescent labeling is the most likely approach by which these cells will be seen.

3.1.5. Henle fibers. Moving deeper into the retina, one study reported an image of purported Henle fibers, which are the elongated axons of cone and rod cells that connect to their tangentially displaced bipolar cells near the fovea (Scoles et al. 2014a). Similar to the NFL, the Henle fiber layer is formed by an array of highly oriented fibers that tend to exhibit strong orientation-dependent scattering characteristics (Lujan et al. 2011). Under normal conditions, Henle fibers do not run perpendicular to the imaging beam and are generally not seen. In the case of Best's vitelliform disease (shown in **Figure 4**), however, the large subretinal lesion has distorted the inner retina, reorienting the fibers and giving rise to sufficient scatter to reveal their structure.

3.1.6. Photoreceptors. Photoreceptors were the first microscopic structures in the retina to be studied using AO, and they have remained the most studied thus far. These cells are of direct interest to researchers, as they comprise the first neurons in the human visual system. Importantly, similar to the bipolar cells, the nuclei of the photoreceptors have not been resolved using an AO system. Rather, AO systems image the light scattered and emitted from the waveguiding portions of the cells (the inner and outer segments); the waveguiding property of cones gives them excellent scattering properties and intrinsic contrast (Roorda & Williams 2002). Advances in ophthalmic AO technology over the years have led to significant improvements in our ability to image these cells, to the point where it is now possible to record clear mosaics of rods and cones across much of the macular region. AO fundus cameras have had moderate success in imaging foveal cones and rods (Doble et al. 2011), but, as evidenced by the images in **Figure 5***a*, confocal AOSLO has been the clear winner in this regard (Dubra et al. 2011).

Although confocal AOSLO has the best spatial resolution of all modalities, the confocal aspect of this technique also limits the information that can be collected, and thus sometimes gives a false impression of retinal structure (see **Figure 13**). Two alternate approaches to imaging the photoreceptor array are shown in **Figure 5***b,c*. **Figure 5***b* shows an image of the peripheral cone
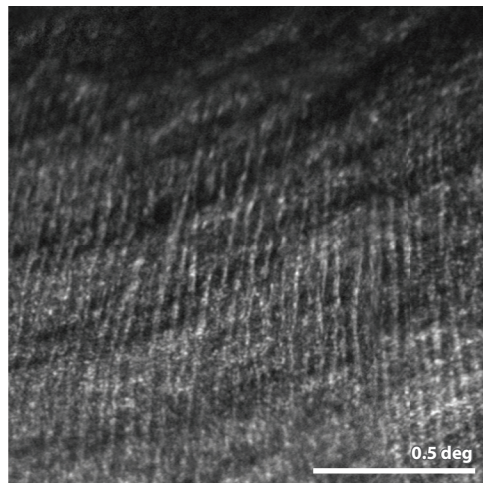
Figure 4

Confocal adaptive optics scanning laser ophthalmoscopy (AOSLO) image of a patient with Best's disease. Purported Henle fibers run vertically across most of the image. The larger, more horizontally oriented structures are from the nerve fiber layer. Figure adapted from Scoles et al. (2014a).

mosaic taken using split-detector AOSLO (Scoles et al. 2014b). The compromise to resolution inherent to this technique results in a failure to resolve the intervening rods (for comparison, see **Figure 5a**), but the cones, or their inner segments, are unambiguous and take on an embossed appearance similar to that of in vitro microscope images using Nomarski optics (Curcio et al. 1990). The fact that this technique does not rely on direct backscattered light (including waveguided light)
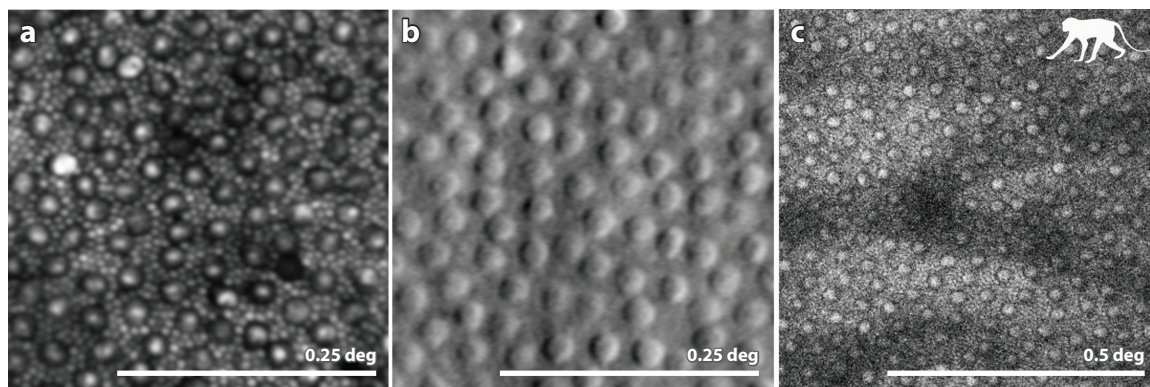

Figure 5

(*a*) Confocal adaptive optics scanning laser ophthalmoscope (AOSLO) image of a healthy human retina showing a complete mosaic of cones (large cells) and rods (intervening smaller cells) at a location 10 deg temporal to the fovea. Panel adapted from Cooper et al. (2011). (*b*) Split-detector AOSLO image of a healthy human retina showing an array of cone inner segments at a location 10 deg from the fovea. Owing to their small size, the rods, which fill the intervening space between the cones at this location, are too small to be resolved. Panel adapted from Scoles et al. (2014b). (*c*) two-photon fluorescence AOSLO image of the retina of a macaque monkey showing the array of photoreceptors (confirmed by taking a confocal AOSLO image at the same location). The appearance of a mosaic in the two-photon image indicates that the fluorophores are contained within the photoreceptor. Image courtesy of J. Hunter, R. Sharma, and D. Williams.

means that these structures might be visible even when the cone is not waveguiding and scattering normally. The potential visibility of these structures may prove useful in identifying whether or not photoreceptor inner segments remain after the outer segments, or other structural features that give rise to the waveguided photoreceptor reflection, are not present. Such a case is reported in **Figure 13**.

Finally, the group in Rochester (Hunter et al. 2011) has managed to acquire images of the cone photoreceptor array in a macaque monkey using two-photon fluorescence imaging of the intrinsic fluorophores in the photoreceptors. The implications of such an image are profound, as the two-photon fluorescence signal indicates the presence of specific molecules in the retina. Resolved in this way, these signals may serve as effective biomarkers for retinal or photoreceptor health. Recent results from that lab have shown significant improvements in efficiency and have expanded the scope of what can be visualized (Sharma et al. 2013), but the approach is not yet ready for use in living human eyes.

3.1.7. Retinal pigment epithelium. The retinal pigment epithelium (RPE) plays a crucial role in retinal health and function, and RPE cells are implicated as the primary affected cell type in several diseases, most notably age-related macular degeneration (AMD). RPE cells are relatively large and fall easily within the resolution limits of the AOSLO system. OCT images also suggest that the RPE layer is a relatively strong backscatterer. However, visualization of these cells has proven difficult for AO fundus cameras and even for confocal AOSLOs. The first reports of visible RPE cells were in selected cases of cone and rod degenerative diseases (Roorda et al. 2007). These reports were working from an idea that in a healthy retina, the strong spatially resolved signal from the photoreceptors masked the relatively weaker scattering from the RPE, allowing the RPE to be revealed only when the photoreceptors were missing. In that case, OCT images from the same locations supported the presence of RPE cells and the lack of photoreceptor cells.

Figure 6a shows an example image of an RPE mosaic taken from a patient with retinitis pigmentosa. In confocal AOSLO, the mosaic is revealed because the scattered light comes from the vicinity of junctions between the cells, whereas the cell centers are hyporeflective. The source of scattered light is not known, but it coincides with lipofuscin accumulation (see **Figure 6b**).

Fundus autofluorescence (FAF) has been used to measure lipofuscin content in the retina, most prevalently in the RPE cells (Delori et al. 1995), and one group discovered that the same fluorescent signal could be used in an AOSLO system to resolve the RPE cells (Morgan et al. 2009). **Figure 6b** shows an image of the RPE mosaic taken from the healthy human retina. Although this technique is less comfortable to the patient and carries the risk of potential phototoxicity (Hunter et al. 2012, Morgan et al. 2008), it offers a distinct advantage in that the FAF signal can be used not only to resolve cells, but also to quantify their molecular content (in this case, the presence of lipofuscin).

Once again, nonconfocal AOSLO detection schemes have recently proven effective to image cells not visible with confocal methods. By blocking the direct backscatter from the waveguiding photoreceptors and by preferentially detecting multiply scattered light, **Figure 6c** shows how dark-field AOSLO imaging can be used to record images of RPE mosaics in healthy human retinas (Scoles et al. 2013). Corresponding confocal AOSLO images recorded simultaneously and at the same location show the overlying photoreceptor mosaic.

3.1.8. Lamina cribrosa. The final structures that benefit from AO imaging are in the region of the optic disk. In particular, AO has been used to reveal the microstructure of the lamina cribrosa (LC), a porous network comprising beams of flexible collagenous tissue that form the passageway for retinal vessels and nerve fibers to enter and leave the eye. Change in the structure of the LC
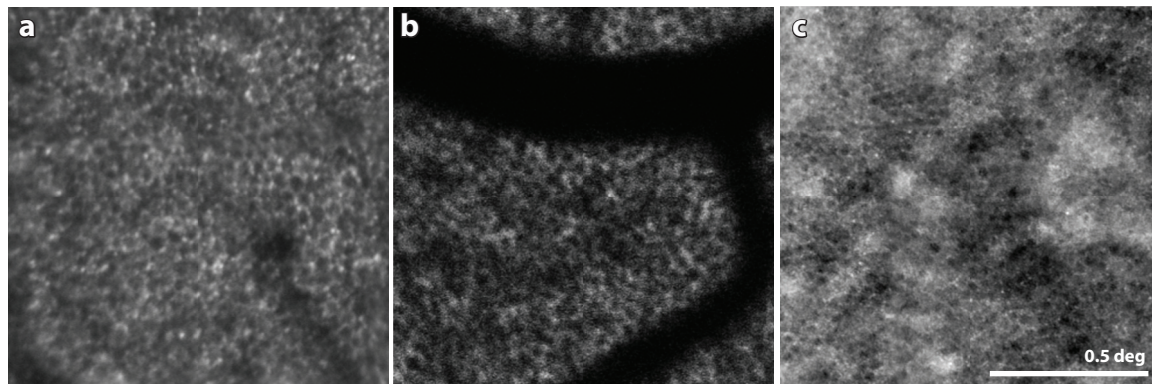
Figure 6

(*a*) Confocal adaptive optics scanning laser ophthalmoscopy (AOSLO) image of the retinal pigment epithelium (RPE) mosaic at a location 3 deg inferior to the fovea in a patient with autosomal dominant retinitis pigmentosa (RP). The lack of overlying visible or functional photoreceptors in this region allowed the RPE cells to be seen. (*b*) AOSLO fundus autofluorescence (FAF) image of a healthy human retina. By resolving the FAF signal, the mosaic of RPE cells is readily visible. The dark shadows in this panel are cast by the overlying blood vessels. The FAF uses short-wavelength light, which is especially susceptible to absorption by the overlying blood vessels (see the subsection titled "Analysis and Interpretation" for more discussion), in both directions. Panel adapted with permission from Morgan et al. (2009). (*c*) Dark-field AOSLO image of a foveal RPE mosaic in a healthy human retina. The same location imaged in confocal AOSLO mode shows a complete mosaic of photoreceptors. Panel adapted with permission from Scoles et al. (2013).

that results from a pressure imbalance is suggested to contribute to ischemia and/or cause axonal damage to the optic nerve, leading to glaucoma. Thus, improved views of this structure may reveal both the mechanical changes that occur and their possible implications for optic nerve health. **Figure 7** shows an example image of the LC from a nonhuman primate retina (Ivers et al. 2011). Although AOSLO lacks the depth resolution and sensitivity of OCT methods to view the LC (for
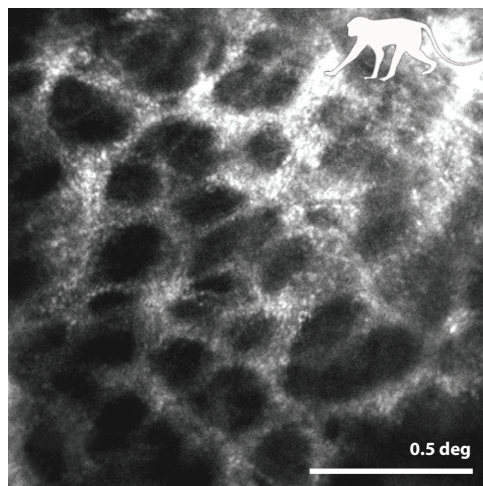

Figure 7

Detailed image of the collagen beams that compose the inner surface of the lamina cribrosa (LC) in a nonhuman primate. Morphometric analysis of LC pore size and pore elongation have been found to be sensitive to changes in ocular pressure in animal models. Figure adapted with permission from Ivers et al. (2011).

comparison, see Nadler et al. 2014, Vienola et al. 2012), this technique generated the highest-resolution images of the LC surface structure ever obtained. Significant changes have been found in LC structural parameters in nonhuman primates with experimentally induced glaucoma (Sredar et al. 2013, Vilupuru et al. 2007) and in humans with glaucoma (Akagi et al. 2012).

3.1.9. Subretinal structures. The previous subsections cover most of the structures in normal eyes that have been visualized using AO ophthalmoscopes. To date, no images of subretinal structures obtained with AO systems have been published, with the exception of some choroidal vascular details seen through geographic atrophy (GA) (this condition offers a window to the choroid and sclera). The main challenge to imaging subretinal structures is the weak signal arising from these layers. A combination of longer wavelengths and heterodyne detection (OCT), possibly with the addition of more innovative collection optics and AO, will likely be the key to imaging subretinal structures at cellular-level resolution.

3.2. Associating Function with Structure

The potential for AO imaging to offer new insights into eye disease and to accelerate efforts to treat it is exciting, but it is important to understand that structural information only tells some of the story. Any assessment of visual health is incomplete unless the functional consequences of the observed structure are understood. This section highlights several ways in which AO has been used to directly measure functional properties of retinal cells. It is divided into two sections: objective and subjective functional tests.

3.2.1. Objective functional tests. Cellular-level retinal photopigment densitometry using single acquired frames has been used to reveal important properties of cone photopigments (Hofer et al. 2005a; Masella et al. 2014a,b; Roorda & Williams 1999). The added dimension of time resolution in AO imaging though the use of video, first with AOSLO (Roorda et al. 2002) and subsequently through a new generation of high-frame-rate AO fundus cameras (Bedggood & Metha 2013, Rha et al. 2006), has broadened the scope of functional vision testing.

Encouraged by the discovery of significant light-induced optical scattering changes in photoreceptors found using an OCT system and an in vitro preparation (Bizheva et al. 2006), several groups used AO to perform similar measures, but with the advantage of improved lateral resolution. Importantly, the source of a detected signal change in systems using incoherent light results only from absorption by the tissue or from changes in its structure and/or refractive index that give rise to changes in the magnitude of the scattered light. In contrast, changes in the detected light signal using coherent or partially coherent light can also arise from interference in systems. The latter signals can be very high contrast, masking the former. Grieve & Roorda (2008) used low-coherence light in a confocal AOSLO setup to look at average scattering changes over time. They used a 30-Hz system and found changes on the order of 5% with multisecond time courses. Three groups have used partially coherent light and high-speed AO fundus cameras to record fast changes in photoreceptor scattering in response to light stimulation. In all cases, significant fluctuations of the light scattered from the photoreceptors were observed. When using partially coherent light (light with coherence lengths less than the twice the length of the photoreceptor outer segments), the source of these signal fluctuation is not well understood (Bedggood & Metha 2012b, 2013; Rha et al. 2006, 2009). However, when imaging with light of longer coherence lengths (greater than twice the length of the outer segments), a useful component of the interference signal that is directly related to the outer segment length can be recorded. Jonnal et al.

(2010) were able to use this signal to measure the growth rate of human cone outer segments. The combination of interferometry and AO was able to reliably measure an impressively slow growth rate of 93–113 nm/h!

To date, intrinsic signals from other, less reflective neurons in the retina have not been observed directly with AO systems. The only functional optical recording from inner retinal neurons using AO has relied on the use of neural activity–dependent fluorescent dyes (calcium indicators, G-CaMP3) in mice (Yin et al. 2013) and in monkeys (Yin et al. 2014). These fluorescence-based approaches are not yet ready for use in humans, but the accelerating development of effective virus-based cellular delivery systems for gene therapy, along with the possibility that these vectors may also be approved to carry fluorescent payloads, means that these techniques may translate to human use sooner than we might have anticipated.

One of the most fruitful objective functional measures has been that of blood flow. Cellular access combined with high frame rate imaging has allowed for better characterization of hemo-dynamics than ever before. **Figure 8** includes a link to a short video from a high-frame-rate AO
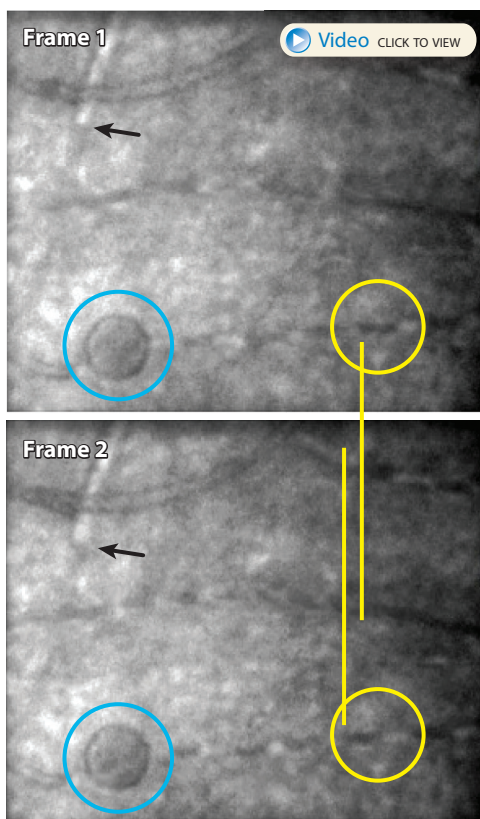

Figure 8

Two subsequent frames of a video of a patient with type 1 diabetes taken using a 400 frame-per-second adaptive optics fundus camera. One of the hyporeflective red blood cells (*yellow circle*) in frame 1 appears displaced to the left in the next frame. A white blood cell in the upper left of each frame (*black arrow*) shows similar movement. The blue circle indicates a microcyst that resides in the same plane as the vasculature. The slow-moving blood cells are much better appreciated in the video. Video courtesy of P. Bedggood and A. Metha, University of Melbourne.

fundus camera; in that video, individual red and white blood cells can be tracked as they move through the capillaries (Bedggood & Metha 2012a). Tam et al. (2011b) used videos taken in an AOSLO system to differentiate between the pathways that white and red blood cells prefer to take through the capillary network, identifying what they called "leukocyte preferred paths." Finally, Zhong et al. (2011) modified their AOSLO to switch between raster and line scan modes. They used the raster scan mode to identify and target blood vessels. Once targeted, switching to the line scan mode enabled extremely high-rate imaging of flow through the larger retinal blood vessels. The ability to measure functional properties of the microvasculature has implications beyond ophthalmic applications: It may offer a new way to study systemic disorders such as Alzheimer's disease and diabetes. We discuss the use of AO to study vasculature in diabetes and other diseases in Section 4.2.

A final objective functional measure is that of fixation stability and eye movements. Having a microscopic image of a living retina means that we can also know the direction that the eye is pointing on the same scale. Putnam et al. (2005) used this property to measure the locus of fixation in a human eye. With the advent of higher-frame-rate AO imaging came the ability to measure fixational eye movements dynamically. In fact, an AOSLO system can track motion at much higher rates than its frame rate by analyzing the small distortions that are present within each acquired frame. Capitalizing on this property, analyses of AOSLO videos have generated the most accurate fixational eye movement statistics ever recorded (Stevenson & Roorda 2005).

The ability to measure eye movements might be useful to diagnose or to better understand some eye diseases and neurological disorders. The ability to track and compensate for the motion of the eye might also make imaging patients with abnormal eye movements, such as nystagmus, easier. Finally, the measurement of eye movement can facilitate functional testing at targeted locations (see Section 3.2.2). Routine eye tracking for the broader clinical population remains a challenge, however, as the field sizes of typical AO systems are small and the movements associated with many eye diseases are relatively large.

3.2.2. Subjective functional tests. AO systems can also be used to control the optical properties of light delivered to the retina. AO for vision correction was used early on to show expected improvements in contrast sensitivity (Liang et al. 1997, Yoon & Williams 2002), but the correlations of structure and function are where the full technology was really demonstrated. Hofer et al. (2005b) used AO-corrected light delivery to study color percepts elicited by stimulation of individual cones. Rossi & Roorda (2010) performed AO-corrected vision tests to study the relationship between cone spacing and acuity at and near the fovea. Finally, Makous et al. (2006) used their AO system to test visibility of brief, cone-sized flashes of light for a subject who, by all appearances in the AO retinal image, had an incomplete cone mosaic. Approximately 1/3 of the cones were not visible in the AO retinal images for this subject, leaving visible gaps in the cone mosaic. Makous et al. inferred from their results that these cone-sized gaps were indeed microscotomas.

As impressive as these early results were, the technology was only able to deliver AO-corrected stimuli; it was not able to target those stimuli to particular cells or specific retinal locations. To overcome those limitations, Roorda and collaborators (Arathorn et al. 2007) built a system that combines AO-imaging, eye tracking, and AO-corrected stimulus delivery to visualize, track, and target individual cells with AO-corrected light stimuli. By performing the imaging and eye tracking in real time, they achieved stimulus delivery with an accuracy of better than 1.3 μm. Further refinements to the image-processing algorithms (Yang et al. 2010) and subsequent development of tools to measure and correct for transverse chromatic aberration (Harmening et al. 2012) culminated in the ability to reliably perform vision testing experiments on single cone photoreceptors (Harmening et al. 2014).

A system with this precise targeting capability holds promise for identifying important structure–function relationships in eye disease (Tuten et al. 2012), in which structural changes can be very focal. Section 4.2 presents a specific example of the use of AO microperimetry for patients with macular telangiectasia type II.

4. HOW IS ADAPTIVE OPTICS SCANNING LASER OPHTHALMOSCOPY BEING USED CLINICALLY?

4.1. Characterization of Eye Disease

The previous sections focused on the capabilities of current AO systems. Over time, we can expect to see many of these new approaches translate to clinical applications. Nevertheless, AO is already having an impact in ophthalmology. The charts in **Supplemental Figure 1** plot publication trends that indicate how AO is being used in ophthalmology today. Three main trends can be drawn from these charts: The total number of published papers continues to increase, AOSLO systems are producing an increasing fraction of papers over time, and clinical applications are accounting for an increasing fraction of these papers over time. Dozens of clinical papers report on the use of AO imaging to better characterize a disease. These are valuable studies, especially those that report on a clinically or genetically well-characterized disease. **Supplemental Table 1** shows a categorized list of ocular diseases with citations to all of the relevant papers that have reported on them using AO systems.

▶ Supplemental Material

4.2. New Discoveries About Eye Disease

Characterization of eye disease is important, and we can expect to see dozens of new papers in this field focusing on numerous diseases. This section discusses three diseases in particular, diabetes, AMD, and macular telangiectasia, and it expands on how AO specifically has been used to make entirely new discoveries or to provide new insights about the mechanisms for these diseases and their progression.

4.2.1. Diabetes and other vascular diseases. Several AOSLO studies of diabetes have made new discoveries. In a cohort of patients with no diabetic retinopathy, Tam et al. (2011a) used confocal AOSLO with motion contrast to perform a series of high-resolution structural and functional analyses of the retinal microvasculature near the fovea. In the patient cohort (diabetes without retinopathy), trends were observed in several metrics, including blood cell velocity, foveal avascular zone (FAZ) size, and capillary density at the edges of the FAZ. These metrics were no different from normal controls, however, possibly because the measurements are variable in a normal population, and too few subjects were enrolled in each cohort to detect a difference. One measurement—that of vessel tortuosity—did show a difference: Capillaries around the FAZ in the diabetic patients were more tortuous than those in the normal population. Tam et al. (2011a) hypothesized that the less tortuous vessels, which serve as the leukocyte preferred paths and transport the majority of white blood cells from arterioles to venules, were lost, leaving the more tortuous capillaries behind. This supposed vessel loss was too small to be detectable as an enlargement of the FAZ or as a reduction of capillary density, for reasons described above, but it emerged in the tortuosity analysis. The loss of the leukocyte preferred paths was suggested to initiate a more rapid degeneration as leukocytes would have to find a new path from arterioles to veins through more tortuous, and consequently more vulnerable, paths.

In a study of patients with mild to moderate nonproliferative diabetic retinopathy, Burns et al. (2014) used offset pupil AOSLO and found significant vessel remodeling, and their setup revealed microvascular abnormalities with exquisite detail. Quantitatively, they found larger than normal capillary diameters (8.2 ± 1.1 versus 6.1 ± 0.75 μm for diabetic and normal retinas, respectively) around the FAZ. In arterioles, they found thicker vessel walls in diabetic versus normal retinas, as quantified by the wall-to-lumen ratio (1.1 ± 0.87 versus 0.42 ± 0.28 μm for diabetic and normal retinas, respectively).

Finally, Dubow et al. (2014) published a study using AOSLO FA to classify a rich and diverse array of microaneurysms in retinas affected by diabetes and other vascular diseases (see **Figure 9a**). In one patient with a central retinal vein occlusion, they showed regression of a microaneurysm in response to treatment with vascular endothelial growth factor (VEGF). A related paper reporting on the same patient presented five different ways in which AO imaging can visualize individual microaneurysms (Chui et al. 2014). **Figure 9b** highlights two microaneurysms that have quite different appearances. These papers make an excellent case for the use of AO imaging to better identify and classify vascular abnormalities and to track changes in vascular structures over time. These highly sensitive measures, which would not have been possible without the resolution and contrast offered in AO systems, can indicate the earliest structural indications of disease and may provide useful biomarkers for disease progression or response to treatment.

4.2.2. Age-related macular degeneration. AMD is a common eye disease and is a leading and significant cause of vision loss among people age 50 and older (**https://www.nei.nih. gov/eyedata/amd**). Although this disease is highly prevalent and extensively studied, the primary affected cells and the nature of its progression remain poorly understood (Lim et al. 2012). Several recent AO studies shed light on this important disease and promise to accelerate efforts to understand and treat it. For example, Zayit-Soudry et al. (2013) measured properties of cones over time in several AMD patients. They showed clear examples of cone disruption over some drusen and in areas of GA, and the cone mosaics in the retinas of AMD patients often exhibited somewhat abnormal reflective characteristics, but no progressive increase in cone spacing that might indicate a steady loss of cones was detected in their longitudinal study of the same regions over 12–21 months. [Compare this result with the progressive loss in cone density and increase in cone spacing for retinitis pigmentosa reported by Talcott et al. (2011).] This result suggests that cone loss is likely to occur as a consequence of other structural changes in AMD, such as the loss of RPE cells in GA. Similarly, Godara et al. (2010) found undisrupted cone mosaics over early drusen. These findings are supported by histology, in which photoreceptor disruptions were seen only over the drusen, not in the areas adjacent to them (Johnson et al. 2003). By comparison, AOSLO studies of cones over reticular pseudodrusen showed earlier and more prevalent loss of cone visibility (Meadway et al. 2014, Zhang et al. 2014), and cones in the surrounding areas had a normal appearance (see **Figure 10**). This loss pattern may result from direct damage to photoreceptors by subretinal drusenoid deposits beneath them, in contrast to the case of typical drusen, which exist beneath RPE cells that could sustain the overlying photoreceptors.

Although photoreceptors may suffer collateral damage from other changes occurring in AMD, the RPE may undergo the earliest structural changes. The autofluorescence images collected with an AOSLO setup and shown in **Figure 11** find disruptions in the uniformity of the RPE layer in AMD patients (Rossi et al. 2013).

Finally, an AO fundus camera was used to visualize and track clumps of melanin granules in the vicinity of GA in patients with AMD (single frame shown in **Figure 12**). Gocho et al. (2013) were the first to observe a dramatic movement of these granules over time, suggesting a potential
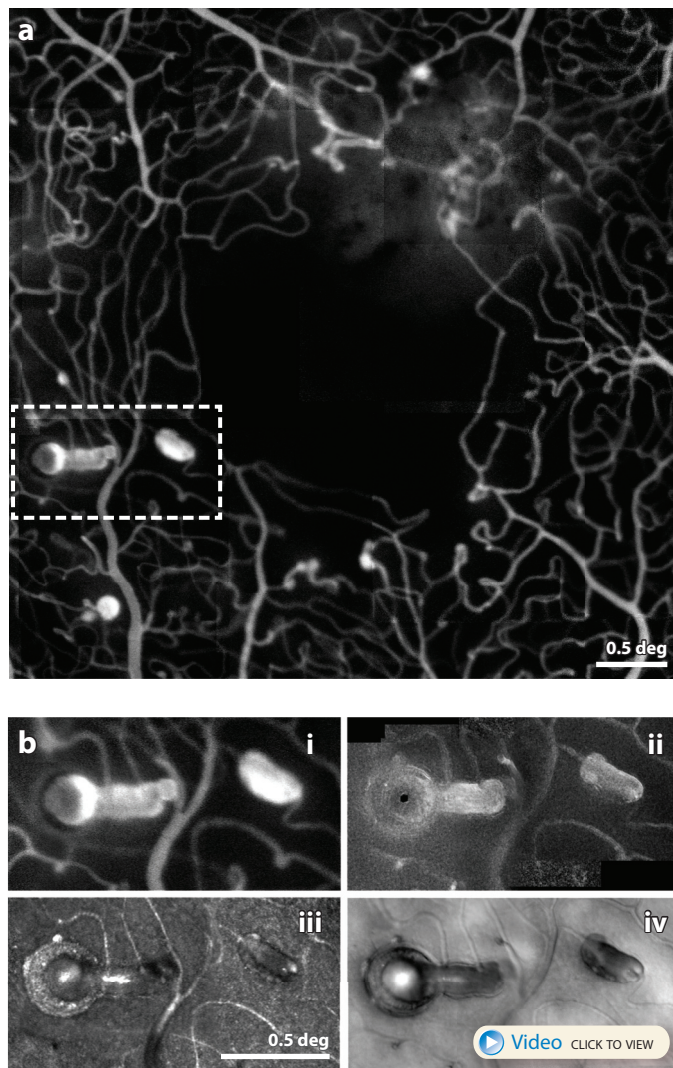
Figure 9

(*a*) Adaptive optics scanning laser ophthalmoscope (AOSLO) fluorescein angiography image of a patient with hypertension. A myriad of microaneurysm types are seen here, as are the fine details of the associated microcapillary network. Panel adapted with permission from Dubow et al. (2014). (*b*) This panel comprises four subpanels, each of which shows a close-up of one location (*dashed white box* in panel *a*) imaged using one of four different modes in the same AOSLO system: (*i*) fluorescein angiography, (*ii*) confocal, (*iii*) motion contrast, and (*iv*) offset pinhole. A video recorded with offset-pinhole AOSLO can be seen by clicking on panel *iv*. Collectively, these images represent the most detailed characterization of single microaneurysm from a human eye in history. Panel adapted with permission from Chui et al. (2014).

important role of melanin in the progression of GA and identifying a possible biomarker for disease progression.

4.2.3. Macular telangiectasia. Macular telangiectasia type 2 (Yannuzzi et al. 2006) is less prevalent than diabetes or AMD, but a recent paper using a combination of AOSLO imaging and AO
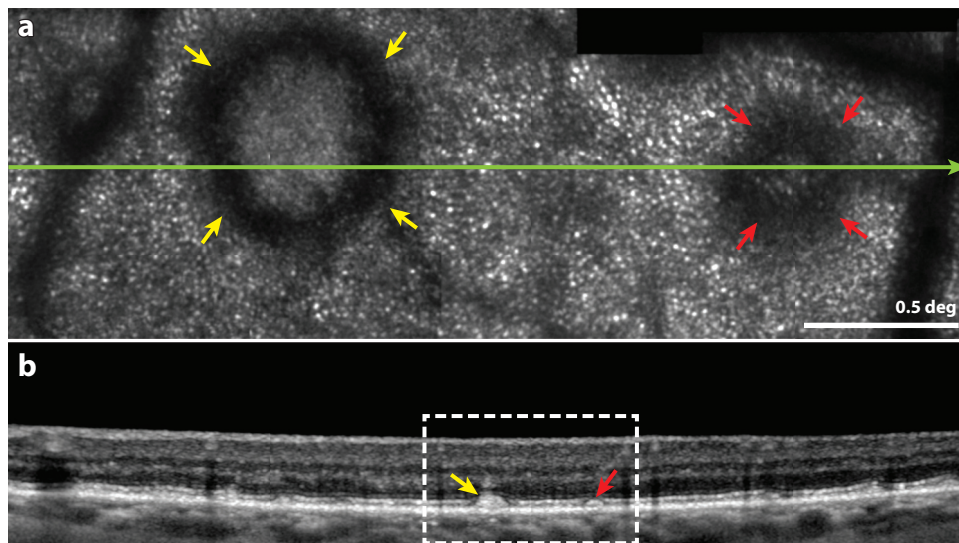
Figure 10

Multimodal imaging of subretinal drusenoid deposits (SDDs, or pseudodrusen) in a patient with age-related macular degeneration. (*a*) Confocal adaptive optics scanning laser ophthalmoscope (AOSLO) image. The yellow and red arrows indicate prominent stage 3 and stage 2 SDDs, respectively, characterized by a hyporeflective ring and no discernible cones over the SDD. Cones that appear to be normal can be resolved outside of the SDD. The green line indicates the location of the optical coherence tomography (OCT) b-scan shown in panel *b*. (*b*) Spectral domain (SD)-OCT b-scan showing a wider field image of the same structure. The dashed white box indicates the region depicted in the AOSLO image in panel *a*. Figure adapted with permission from Zhang et al. (2014).
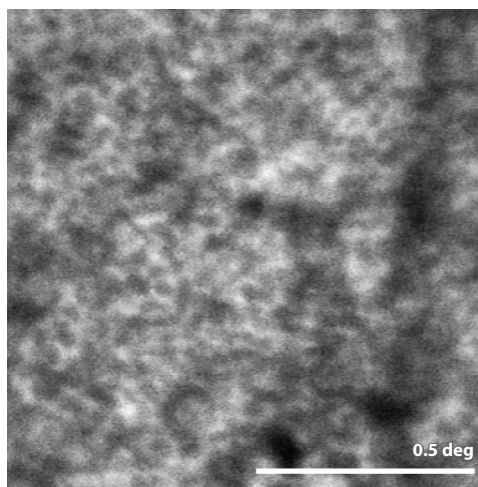

Figure 11

Adaptive optics scanning laser ophthalmoscope autofluorescence image of the retinal pigment epithelium (RPE) mosaic in a patient with age-related macular degeneration (AMD). Analysis of this mosaic, and of other mosaics from AMD patients, showed that the RPE regularity is disrupted in this disease. Figure adapted with permission from Rossi et al. (2013).
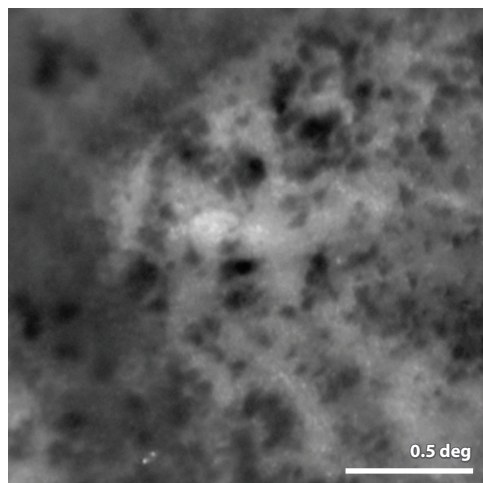
Figure 12

Image of melanin granules taken with an adaptive optics fundus camera (rtx1, Imagine Eyes Inc., Orsay, France). The granules (*dark regions*) are readily visible in age-related macular degeneration patients in the vicinity of geographic atrophy (*lighter background regions*); the authors report that these granules are highly active, appearing, disappearing, and moving many micrometers over the course of weeks. Figure adapted with permission from Gocho et al. (2013).

microperimetry highlights two discoveries that might prove relevant to many retinal degenerative diseases (Wang et al. 2015). Patients with early stages of macular telangiectasia can present with small discrete lesions in the photoreceptor layer close to fixation. Outside of these lesions, cones appear to be relatively normal. When tracking these lesions over time, Wang et al. (2015) found that although the overall size of the lesions expanded, some areas showed recovery of normally reflecting cones. Cone spacing measurements indicated that these recovered cones had normal spacing. As it is unlikely that new cones were generated, these cones probably were present throughout the study but were lacking the physical structure that gave rise to a visible reflection. To investigate further, the group used AO microperimetry to measure the visual function of the recovered cones as well as at other targeted regions across the lesion. They found normal sensitivity in the recovered cones and measureable, but reduced, function in parts of the lesion that appeared to be devoid of cones in both OCT and confocal AOSLO. Previous studies using OCT have reported recovery of the inner and/or outer segment reflection in some diseases, and those using AOSLO have reported recovery of cones (Ooto et al. 2011, 2012), but the study by Wang et al. (2015) is the first to report both functional and structural recovery of a clear and unambiguous array of cones. It is also the first definitive measure of visual function in a region in which AO imaging would otherwise have suggested a complete lack of cones.

This study reinforces the notion that one must be cautious about inferring function directly from structure. It also highlights the need for new imaging methods to reveal structure. For example, split-detector AOSLO imaging was not available for this study, but, had it been used, it might have found a complete mosaic of inner segments in both the part of the lesion that retained visual function and the part that recovered normal reflectivity. The study also lends support to the idea that recoverable cones might exhibit a characteristic appearance with OCT (Chhablani et al. 2012, Landa et al. 2012). The specific characteristic in question is the preservation of the external limiting membrane above relatively transparent (dark) tissue in the region in which reflections

consistent with the inner and/or outer segments and the posterior tips of the outer segments are normally seen.

4.3. Adaptive Optics as a Tool for Clinical Trials

Perhaps the most immediate benefit of AO will be in evaluating new treatments to cure, prevent, or slow the progression of eye disease. The ability of an AO ophthalmoscope to resolve cells and return to the same cells day after day offers the ability to track disease progression on an unprecedented cellular scale. Measuring disease progression on this scale has normally been possible only in animal models and required sacrificing animals with and without treatment at various stages of disease progression. AO offers two advantages: First, the microscopic imaging can be done noninvasively in humans. Second, imaging the same cells in the same human eye longitudinally reduces noise caused by differences in treatment response between individual patients, possibly making clinical trials more efficient and conclusive.

To date, the only published report in which AO images of photoreceptors were used to evaluate disease progression and response to an experimental treatment for retinal degeneration was one by Talcott et al. (2011), in which the efficacy of using ciliary neurotrophic factor (CNTF) to treat patients with retinitis pigmentosa was evaluated. Analysis of a subset of three participants from a larger, multicenter Phase 2 clinical trial in which one eye was treated with CNTF and the fellow eye served as a control showed a significant difference: The cone density declined less rapidly in the treated eye compared with the fellow eye over 24–32 months. Although assessing whether a treatment is working involves much more than simply monitoring the preservation of visible cones, AO technology offers the potential to make the path of drug development for eye disease faster and more cost effective. Currently, quantitative measures from AO images are being employed as primary and adjunct outcomes in three known clinical trials involving a treatment. The first is a larger trial studying cone photoreceptor spacing as the primary outcome measure in response to CNTF treatment of 30 patients with retinal degeneration and is currently enrolling patients (**http://www.clinicaltrials.gov**, trial NCT01530659). A second, similar CNTF trial is underway for the treatment of macular telangiectasia type 2 (**http://www.clinicaltrials.gov**, trial NCT01949324). Longitudinal measures of cone spacing and cone coverage are being collected in an ancillary study within this trial. Finally, photoreceptor survival as assessed from AO images will also be used to provide a secondary outcome in a Pfizer-sponsored stem cell therapy trial for AMD currently being conducted at University College London (**http://www.clinicaltrials.gov**, trial NCT01691261).

4.4. Prescreening for Suitable Patients

This is an exciting time in the battle to treat and cure retinal degenerative disease. Gene therapy trials (Bainbridge et al. 2008, Hauswirth et al. 2008, Maguire et al. 2008), retinal prosthetics (Weiland et al. 2011), and stem cell therapies (Schwartz et al. 2012, Schwartz et al. 2015) are all showing promising results. And, thanks to the National Eye Institute Audacious Goals Initiative to "Regenerate Neurons and Neural Connections in the Eye and Visual System" (**http://www. nei.nih.gov/audacious/**), the ability to offer solutions to patients with previously untreatable diseases is now more likely than ever to become a reality. However, careful identification of the diseases that are amenable to treatment will be especially important in the early stages of this effort, as will identification of patients who are at a stage of progression that is most amenable to treatment. Microscopic AO imaging will likely play an important role in screening which patients are most likely to benefit.

Achromatopsia is an excellent example of a disease whose treatment success may benefit from improved screening. Achromatopsia is a rare condition, affecting 1 in 30,000 individuals, but it is particularly relevant to this discussion as it is slated for gene therapy trials in the near future (**http://www.achromacorp.org/PathToCure.html**). It is present at birth or in early infancy, and its symptoms include reduced acuity, photophobia, complete lack of or reduced color vision, and nystagmus. Electroretinogram (ERG) measurements show a loss of cone function but normal rod function. Mutations in the *CNGA3* and *CNGB3* genes, which encode aspects of cone phototransduction, account for approximately 70% of achromatopsia cases (Kohl et al. 2005).

Although the gene is known, the prospects for whether gene therapy will benefit this condition depend on the state of the retina. If a cone is present but dysfunctional, the prognosis is much better than if the cone has degenerated completely. In fact, OCT studies have shown that achromatopsia patients suffer varying degrees of degeneration. Sundaram et al. (2014) suggested that cones are indeed present in some cases but not in others. The first AO studies of this disease showed a marked lack of reflection in the regions in which cones would normally reside, leaving holes in the cone mosaic (Genead et al. 2011). More recently, the use of split-detector AOSLO imaging revealed mosaics of intact inner segments in the regions in which confocal AOSLO images showed hyporeflectivity in the same locations (see **Figure 13**). This very specific finding is the perhaps the best indication for recoverable cones (Dubis et al. 2014), namely, those in which restoration of the nonmutated gene stands a good chance of restoring their complete structure and function.

4.5. Early Diagnosis

Dozens of published reports on AO ophthalmoscopy tout early detection and diagnosis of eye disease as one of the key benefits of the technology, yet no reports have been published in which such an early detection or diagnosis has been made. This is not surprising, given that AO ophthalmoscopy is an emerging technology and that studies to validate the reliability and significance of the findings observed in AO images are ongoing. These new views of the retina require careful
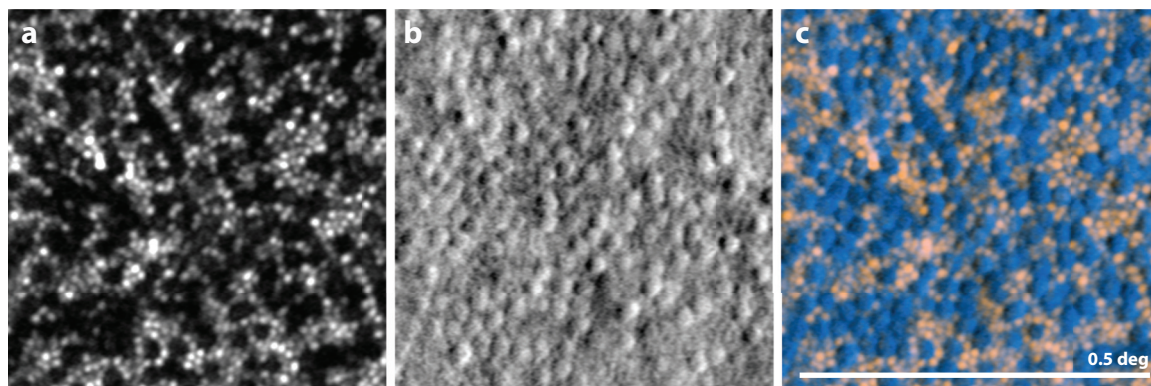

Figure 13

Images showing the value of split-detector imaging for prescreening patients. All images are from the same location of a single patient with achromatopsia. (*a*) Confocal adaptive optics scanning laser ophthalmoscopy (AOSLO) image. Holes (*black*) are present where the cones might normally reside. The visible spots (*gray* and *white dots*) are from intact functional rods. (*b*) Split-detector AOSLO image showing a mosaic of structures, presumably the inner segments of the cones. (*c*) Overlay of the confocal image (*pink*) with the split-detector image (*blue*), revealing that the mosaic of cells corresponds directly with the gaps in the mosaic from panel *a*. In this case, it appears that although the cones are dysfunctional in this patient, a mosaic of inner segments is present. It has been suggested that patients with this phenotype are most likely to benefit from gene therapy. Figure adapted with permission from Scoles et al. (2014b).

interpretation (see Section 5), and most ophthalmologists are unfamiliar with them. Nevertheless, as known diseases continue to be characterized and new microscopic phenotypes continue to be discovered, AO imaging will be used to characterize the earliest stages of these diseases. Moreover, the massive growth in our understanding of the genetics of eye disease suggests that it is just a matter of time before cohorts of subjects with well-known risk factors for eye disease will be studied and followed with AO imaging prior to developing any clinical symptoms. In addition, natural history studies of disease progression that include AO images will demonstrate the sensitivity and validity of this imaging technology. Finally, as treatments emerge, the importance of early diagnosis will increase.

NIR: near-infrared

5. DISCUSSION

The results presented in this review aimed to show the promise of AO and associated technologies for clinical applications. By all indications, AO will become increasingly important in ophthalmology. In terms of optical quality, the most recent results suggest that AO ophthalmoscopes—at least for normal eyes—have achieved the diffraction limit (Dubra et al. 2011). Nevertheless, many potential improvements to these systems could make them more robust for patients. Seemingly minor improvements such as better fixation targets, better pupil and head alignment, and simpler operation will help reduce imaging times and make these systems more useable by any ophthalmic technician. Hopefully, manufacturers of commercial AO systems will be able to help the field by solving many of the ergonomic problems. The real future technical advances in AO imaging, as suggested by so many of the examples we have selected, will be in how AO is used. For example, OCT systems, which are not part of this review, can benefit tremendously from AO. Impressive work in this field is already underway in several labs (Felberer et al. 2014, Jonnal et al. 2012, Zawadzki et al. 2014, Zawadzki et al. 2009).

5.1. Analysis and Interpretation

Perhaps the most important area in which advances can be made is in the analysis and interpretation of retinal images. A careless or unprincipled interpretation of an AO image can lead to erroneous conclusions. Such conclusions will not only compromise our collective understanding of a disease, but they will diminish the perceived value of AO technology. A proper analysis and interpretation begins with a strong understanding of the imaging system and how it interacts with the retina. In the following subsections, we offer a systematic approach to understanding and interpreting images from AO ophthalmoscopes.

5.1.1. Understand the imaging modality. Every imaging modality is designed to record a specific type of signal, and failing to understand the implications of this can lead to erroneous interpretations. **Figure 14** shows a striking example of differences in how images of melanin pigment appear when taken using five different modalities. In a color fundus photograph, melanin clumps appear dark and brownish. In OCT, they are hyperreflective. Similar hyperreflectivity is seen in AOSLO images in near-infrared (NIR) light. However, an NIR AO fundus camera sees the melanin pigment as dark. The hyperreflectivity of melanin granules is what makes them appear bright in OCT and NIR AOSLO; in a full-field AO fundus camera, however, this reflectivity seems to be offset by an even greater one integrated from all depths of the surrounding retinal structure, thereby giving the same granules negative contrast.

A deep understanding of the imaging modality can lead to innovative adaptations of it. For example, confocal AOSLO effectively detects direct backscattered light from the plane of focus.
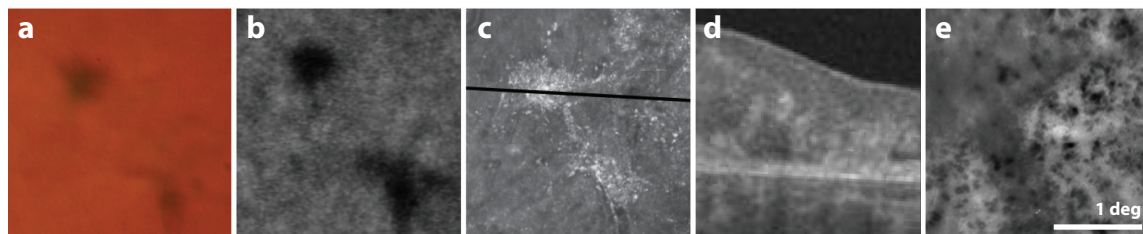
Figure 14

Images of melanin pigment taken using five different imaging modalities. Panels *a–d* show registered images from a single patient with idiopathic macular telangiectasia type 2, panel *e* is cropped from the image of an age-related macular degeneration (AMD) patient with geographic atrophy shown in **Figure 12**. (*a*) Color fundus photo: pigment appears dark and brownish in color. (*b*) Fundus autofluorescence from a Heidelberg SPECTRALIS®: pigment appears dark. (*c*) Adaptive optics scanning laser ophthalmoscopy: pigment is hyperreflective in near-infrared (NIR) (840 nm) light. (*d*) Optical coherence tomography (OCT) b-scan (scan location indicated by the *black line* in panel *c*): pigment is hyperreflective in NIR light. (*e*) Adaptive optics fundus photography: pigment is hyporeflective. Panel *e* adapted with permission from Gocho et al. (2013).

Thus, offsetting or enlarging the confocal pinhole or selectively blocking the confocal light and detecting the light outside of the confocal aperture can preferentially detect multiply scattered light. AO offers exquisite control of the optics, allowing for equally precise control of the how the light is detected. As such, alternate AOSLO detection schemes such as offset pinhole AOSLO (Chui et al. 2012), dark-field AOSLO (Scoles et al. 2013), and split-detector AOSLO (Scoles et al. 2014b) are poised to have a major impact on the field.

5.1.2. Understand the optical role of the retina and how it interacts with the imaging modality. The retina comprises a diverse group of optically active structures. Absorption and scattering by the blood vessels, for example, cast shadows into the deeper retinal layers, especially when using short-wavelength light (see **Figure 6b** for an example). The characteristic structure of the vasculature makes identification of these structures as shadows and not actual scattering changes easy in the deeper layers, but this distinction may not be as obvious in the case of microaneurysms (Ooto et al. 2013) unless one takes a multimodal approach (see Section 5.1.3.).

The waveguiding cones are another example. Cones and rods are optical fibers, and their axes typically point toward the center of the pupil. The small reflection from a healthy cone (maybe 1% at most) is efficiently guided back toward the pupil, making the cone readily visible in a properly focused AO retinal image. If the cone is not aligned properly, however, it will no longer be an efficient backreflector. Although improper alignment is unlikely to explain the variation in cone reflectivity seen in typical AO images from normal eyes (Roorda & Williams 2002), it is likely one of the reasons why cones at the edge of drusen appear dark (see **Figure 10**). Nevertheless, a failure to visualize a cone does not immediately imply a missing cone or even a lack of cone function (see Section 4.2 or Wang et al. 2015). The reflection from a cone might be weak, and the dynamic range of the camera might not be high enough to detect it, but the dynamic range of light sensitivity in humans can be very high (Rodieck 1998).

The regular arrangement of fibers in the NFL, as well as that in the Henle fiber layer (HFL), gives rise to strong backscatter for light that is normally incident to their surfaces. This property makes the NFL highly visible in confocal AOSLO and in OCT. The HFL has the same scattering properties as the NFL but is less visible because the fibers do not run tangential to the retinal surface. **Figure 4** shows that in cases in which retinal pathology deforms these structures, they can become visible.

Most of the inner retinal cells (ganglion cells, Müller cells, bipolar cells, photoreceptor nuclei) are transparent by design and have not been seen directly with AO imaging. Phase-sensitive approaches that have already revealed otherwise transparent inner segments, such as split-detector AOSLO (see **Figures 5b** and **13**), might find some success for other transparent retinal cells.

In contrast to the inner layers of the retina, the RPE and other subretinal structures are highly absorptive and multiply scattering. Thus, confocal detection approaches are generally not suitable for these structures. The best images of deep retinal layers will come from systems that are more sensitive to weak signals (e.g., OCT), use longer wavelengths (e.g., 1060 nm) to reduce effects of multiple scattering and avoid absorption by melanin, preferentially detect a depolarization signal, or use nonconfocal AOSLO detection.

A better understanding of retinal optics (Putnam et al. 2010) offers an opportunity to take advantage of them. For example, the cone photoreceptor contains two relatively discrete reflections: one from near the inner segment–outer segment junction and one from the cone outer segment tips (COST) (Jonnal et al. 2014). When light of the proper coherence length is used, these two reflections become mutually coherent (an optical condition that allows them to constructively or destructively interfere with each other), in effect forming a local interferometer. Jonnal et al. (2010) capitalized on this feature to measure the growth rate of outer segments.

5.1.3. Use multimodal imaging whenever possible. As any single imaging modality has only a limited ability to reveal retinal structure or function, it is useful to integrate the results from multiple modalities whenever possible. This integration is especially important for new technologies, for which there is often far less amassed experience in reading and interpretation of the images. As a simple example, multimodal systems that integrate wide-field fundus views for identifying specific regions of interest and then targeting high-resolution imaging to those regions are proving to be very useful in a clinical setting (Huang et al. 2012). But the advantages of multimodal systems go far beyond the obvious ergonomic benefits. The combination of OCT and AO ophthalmoscopes (SLO or AO fundus cameras) is an excellent example. **Figure 10** shows how two modalities combined reveal a unique phenotype associated with reticular pseudodrusen.

To make the best use of multimodal information, accurate registration of the images from different modalities is very important. This idea is not new; the Heidelberg SPECTRALIS®, among other commercial systems, is an example of excellent integration of SLO and SD-OCT. Similar efforts in modern AO research labs are demonstrating the benefits of multimodal imaging on a microscopic scale (Felberer et al. 2014).

In microscopy, specific fluorescent labels are commonly used to colocalize targets within and between cells, and the information they provide is extremely valuable. Analogous approaches are only beginning to be applied to ophthalmoscopy. Although the scale of colocalization in the retina is much coarser than in other tissues, the knowledge gained will be just as useful, and the colocalized measures can also be more diverse, incorporating structural, molecular, and functional information. This review contains six examples of colocalization: **Figure 3d**, which shows pericytes and perfused capillaries; **Figure 9**, which shows four different modes of AOSLO imaging (five including the movie); **Figure 10**, which shows AOSLO and OCT; **Figure 13**, which shows split-detector and confocal AOSLO; and **Figure 14**, which shows images from a color fundus camera, fundus autofluorescence, confocal AOSLO, OCT, and an AO fundus camera.

5.1.4. It is safer to make conclusions about what can be seen in an image than about what cannot. As mentioned previously, all imaging modalities are limited in terms of the phenomena that they record. This is both good and bad. FA, for example, detects fluorescent light coming from dye injected into the bloodstream, thereby serving to enhance contrast. Also, confocal AOSLO is

sensitive only to direct backreflections from the plane of focus, enhancing contrast and subserving optical sectioning. These technologies, by design, do not detect other aspects of the signal. The fact that neither of these modalities visualizes the RPE cells does not mean that the RPE cells are absent. Dark-field AOSLO, by comparison, does not show photoreceptors but does show the RPE mosaic (see **Figure 6c** or refer to Scoles et al. 2013). To date, none of the modalities mentioned above has visualized ganglion cells, but no one would suggest that these cells are not present. Perhaps the best example of something that is not seen is in achromatopsia, where holes in the cone mosaic seen with confocal AOSLO are readily seen as a mosaic of inner segments using split-detector AOSLO imaging (see **Figure 13**). For this reason, judicious use of multiple modalities to assess retinal structure and function often helps researchers to make conclusions about the presence or absence of cells.

Consider the example of cone density, a seemingly simple measure of the number of cones per unit area. An accurate measurement of cone density requires that every single cone in the selected area be identified. If an obscuration within the inner retinal layers renders the underlying cones dark, then a decision to not consider these regions as containing potential cones will lead to a measurement artifact of reduced density. In patients with retinal disease, subtle disruptions of the inner retinal structure are common and can give rise to deep shadows in the layers of the retina. A more conservative approach might be to measure cone spacing, which is less prone to these artifacts if computed correctly (Duncan et al. 2007).

5.1.5. Determine whether a given image is a bad image of a healthy retina or a good image of a diseased retina. This problem remains unsolved in the field of AO imaging, even though AO ophthalmoscopes have access to more information that can bear on the quality of an image than any other imaging modality does. The AO control loop generally aims to minimize the wavefront errors, and continuously recorded metrics such as the residual wavefront aberration error can potentially be used as indicators of the quality of the correction. If undetectable aberrations such as those caused by tear film changes or cataracts remain, however, the aberration correction might be far worse than the AO system is reporting. Also, the focus setting of an AO ophthalmoscope is generally decoupled from the AO control, so a system with a perfect AO correction could still generate a poor image resulting from improper focus on the structures of interest.

The best approach to assessing the quality of the image ultimately has to reside in the image itself. Image quality metrics such as standard deviation or contrast will be useful (Larocca et al. 2013, Sulai & Dubra 2014). In confocal AOSLO imaging, gauging the magnitude of light detected through the pinhole is a simple and effective strategy (Hofer et al. 2011, Li et al. 2009), although this strategy has some shortcomings (Sulai & Dubra 2014).

5.1.6. Use automated image analysis tools with caution. AO systems can collect a tremendous amount of data in a short period of time, resulting in a profound need for automated methods to generate and analyze images. Automated systems to assemble montages (collections of AO images that have been stitched together to form larger images) are already being developed and used (Huang et al. 2012), but the scope for automation goes far beyond that.

By far, the bulk of the automation effort in AO ophthalmoscopy has focused on automatic identification of photoreceptors from AO images. Not only are the photoreceptors the most commonly imaged structures, but also, photoreceptor metrics such as density, spacing and regularity have been used for decades to understand many aspects of vision, from acuity (Geller et al. 1992, Hirsch & Curcio 1989) to degenerative eye disease (Milam et al. 1998). Several cell-counting algorithms have been developed and improved upon, and these algorithms are regularly used (Chiu et al. 2013, Cooper et al. 2013, Li & Roorda 2007, Xue et al. 2007). By all indications, these algorithms

are very effective for identifying cones in good images from normal eyes. However, the success of these algorithms should never be assumed to have concomitant success with diseased eyes. Aside from a few filters designed to avoid impossible events such as finding cones that are too close together, these algorithms do little more than detect bright spots in an image. They are just as likely to detect "cones" in a speckly image of the NFL or within the bright light reflected from an area of GA as they are to find actual cones.

Therefore, current automated approaches to identify cones should be used with caution, if at all, for studying patients. If the algorithms described above are used, then employing a multimodal approach to provide additional evidence that cones are present (for example, by confirming that the reflections associated with cones are seen in the same region using OCT) is a wise course of action.

6. CONCLUSIONS

Over the past 25 years, we have witnessed tremendous advances in the field of ophthalmoscopy, and this review provides a snapshot of the part that AO has played during this period. History reminds us that we cannot anticipate future developments, so it is risky to predict exactly how AO will be employed in ophthalmoscopy, even in the next decade. AO is not a stand-alone technology, however; it is a general approach that offers microscopic optical access to the retina of a living eye. Thus, similar to other enabling technologies (digital cameras, light sources, faster signal processing), AO will certainly continue to play a role in future developments in ophthalmoscopy in our lifetimes.

SUMMARY POINTS

1. AO technology can be used as an adjunct to any ophthalmic imaging technique. To date, AO has been used in fundus cameras, confocal scanning laser ophthalmoscopes, microperimetry systems, and OCT systems.

2. AO is useful not only for conventional scattered-light imaging, but also for other imaging approaches. Examples include confocal, fluorescence, and phase-sensitive imaging.

3. Researchers have used AO systems to resolve cones, rods, microvasculature, red blood cells, leukocytes, RPE cells, and nerve fibers in humans. In animals, fluorescence-based AO systems have also been used to resolve ganglion cells and to measure their function.

4. AO systems are being used to make new discoveries about vision in healthy and diseased eyes.

FUTURE ISSUES

1. The translation of innovative imaging methods from microscopy to AO ophthalmoscopy will continue to expand the scope of imaging applications. Examples include, but are not limited to, structured illumination, fluorescence lifetime imaging, Raman spectroscopy, and hyperspectral imaging.

2. The lack of reliable automated imaging analysis tools remains a barrier for moving AO ophthalmoscopy into more mainstream clinical use.

3. The ability of AO ophthalmoscopes to image at a cellular level over time ensures that these systems will continue to prove useful for clinical trials involving the testing of new therapies for treating eye disease.

4. AO ophthalmoscopy will continue to make steps toward the imaging of functional and metabolic activity of cells, thereby making more sensitive measures of retinal health.

DISCLOSURE STATEMENT

ACKNOWLEDGMENTS

LITERATURE CITED

Akagi T, Hangai M, Takayama K, Nonaka A, Ooto S, Yoshimura N. 2012. In vivo imaging of lamina cribrosa pores by adaptive optics scanning laser ophthalmoscopy. *Investig. Ophthalmol. Vis. Sci.* 53:4111–19

Arathorn DW, Yang Q, Vogel CR, Zhang Y, Tiruveedhula P, Roorda A. 2007. Retinally stabilized cone-targeted stimulus delivery. *Opt. Express* 15:13731–44

Bainbridge JW, Smith AJ, Barker SS, Robbie S, Henderson R, et al. 2008. Effect of gene therapy on visual function in Leber's congenital amaurosis. *N. Engl. J. Med.* 358:2231–39

Bedgood P, Metha A. 2012a. Direct visualization and characterization of erythrocyte flow in human retinal capillaries. *Biomed. Opt. Express* 3:3264–77

Bedgood P, Metha A. 2012b. Variability in bleach kinetics and amount of photopigment between individual foveal cones. *Investig. Ophthalmol. Vis. Sci.* 53:3673–81

Bedgood P, Metha A. 2013. Optical imaging of human cone photoreceptors directly following the capture of light. *PLOS ONE* 8:e79251

Bizheva K, Pflug R, Hermann B, Povazay B, Sattmann H, et al. 2006. Optophysiology: depth-resolved probing of retinal physiology with functional ultrahigh-resolution optical coherence tomography. *PNAS* 103:5066–71

Burns SA, Elsner AE, Chui TY, VanNasdale DA Jr, Clark CA, et al. 2014. In vivo adaptive optics microvascular imaging in diabetic patients without clinically severe diabetic retinopathy. *Biomed. Opt. Express* 5:961–74

Chhablani JK, Kim JS, Cheng L, Kozak I, Freeman W. 2012. External limiting membrane as a predictor of visual improvement in diabetic macular edema after pars plana vitrectomy. *Graefe's Arch. Clin. Exp. Ophthalmol.* 250:1415–20

Chiu SJ, Lokhnygina Y, Dubis AM, Dubra A, Carroll J, et al. 2013. Automatic cone photoreceptor segmentation using graph theory and dynamic programming. *Biomed. Opt. Express* 4:924–37

Chui TYP, Dubow M, Pinhas A, Shah N, Gan A, et al. 2014. Comparison of adaptive optics scanning light ophthalmoscopic fluorescein angiography and offset pinhole imaging. *Biomed. Opt. Express* 5:1173–89

Chui TYP, Gast TJ, Burns SA. 2013. Imaging of vascular wall fine structure in the human retina using adaptive optics scanning laser ophthalmoscopy. *Investig. Ophthalmol. Vis. Sci.* 54:7115–24

Chui TYP, VanNasdale DA, Burns SA. 2012. The use of forward scatter to improve retinal vascular imaging with an adaptive optics scanning laser ophthalmoscope. *Biomed. Opt. Express* 3:2537–49

Cooper RF, Dubis AM, Pavaskar A, Rha J, Dubra A, Carroll J. 2011. Spatial and temporal variation of rod photoreceptor reflectance in the human retina. *Biomed. Opt. Express* 2:2577–89

Cooper RF, Langlo CS, Dubra A, Carroll J. 2013. Automatic detection of modal spacing (Yellott's ring) in adaptive optics scanning light ophthalmoscope images. *Ophthalmic Physiol. Opt.* 33:540–49

Curcio CA, Sloan KR, Kalina RE, Hendrickson AE. 1990. Human photoreceptor topography. *J. Comp. Neurol.* 292:497–523

Delori FC, Dorey CK, Staurenghi G, Arend O, Goger DG, Weiter JJ. 1995. In vivo fluorescence of the ocular fundus exhibits retinal pigment epithelium lipofuscin characteristics. *Investig. Ophthalmol. Vis. Sci.* 36:718–29

Doble N, Choi SS, Codona JL, Christou J, Enoch JM, Williams DR. 2011. In vivo imaging of the human rod photoreceptor mosaic. *Opt. Lett.* 36:31–33

Dubis AM, Cooper RF, Aboshiha J, Langlo CS, Sundaram V, et al. 2014. Genotype-dependent variability in residual cone structure in achromatopsia: toward developing metrics for assessing cone health. *Investig. Ophthalmol. Vis. Sci.* 55:7303–11

Dubow M, Pinhas A, Shah N, Cooper RF, Gan A, et al. 2014. Classification of human retinal microaneurysms using adaptive optics scanning light ophthalmoscope fluorescein angiography. *Investig. Ophthalmol. Vis. Sci.* 55:1299–309

Dubra A, Sulai Y. 2011. Reflective afocal broadband adaptive optics scanning ophthalmoscope. *Biomed. Opt. Express* 2:1757–68

Dubra A, Sulai Y, Norris JL, Cooper RF, Dubis AM, et al. 2011. Noninvasive imaging of the human rod photoreceptor mosaic using a confocal adaptive optics scanning ophthalmoscope. *Biomed. Opt. Express* 2:1864–76

Duncan JL, Zhang Y, Gandhi J, Nakanishi C, Othman M, et al. 2007. High-resolution imaging with adaptive optics in patients with inherited retinal degeneration. *Investig. Ophthalmol. Vis. Sci.* 48:3283–91

Felberer F, Kroisamer J-S, Baumann B, Zotter S, Schmidt-Erfurth U, et al. 2014. Adaptive optics SLO/OCT for 3D imaging of human photoreceptors in vivo. *Biomed. Opt. Express* 5:439–56

Fernández EJ, Prieto PM, Artal P. 2009. Binocular adaptive optics visual simulator. *Opt. Lett.* 34:2628–30

Geller AM, Sieving PA, Green DG. 1992. Effect on grating identification of sampling with degenerate arrays. *J. Opt. Soc. Am. A* 9:472–77

Genead MA, Fishman GA, Rha J, Dubis AM, Bonci DM, et al. 2011. Photoreceptor structure and function in patients with congenital achromatopsia. *Investig. Ophthalmol. Vis. Sci.* 52:7298–308

Geng Y, Dubra A, Yin L, Merigan WH, Sharma R, et al. 2012. Adaptive optics retinal imaging in the living mouse eye. *Biomed. Opt. Express* 3:715–34

Geng Y, Greenberg KP, Wolfe R, Gray DC, Hunter JJ, et al. 2009. In vivo imaging of microscopic structures in the rat retina. *Investig. Ophthalmol. Vis. Sci.* 50:5872–79

Geng Y, Schery LA, Sharma R, Dubra A, Ahmad K, et al. 2011. Optical properties of the mouse eye. *Biomed. Opt. Express* 2:717–38

Gocho K, Sarda V, Falah S, Sahel JA, Sennlaub F, et al. 2013. Adaptive optics imaging of geographic atrophy. *Investig. Ophthalmol. Vis. Sci.* 54:3673–80

Godara P, Siebe C, Rha J, Michaelides M, Carroll J. 2010. Assessing the photoreceptor mosaic over drusen using adaptive optics and SD-OCT. *Ophthalmic Surg. Lasers Imaging* 41:S104–8

Gray DC, Merigan W, Wolfing JI, Gee BP, Porter J, et al. 2006. In vivo fluorescence imaging of primate retinal ganglion cells and retinal pigment epithelium cells. *Opt. Express* 14:7144–58

Grieve K, Roorda A. 2008. Intrinsic signals from human cone photoreceptors. *Investig. Ophthalmol. Vis. Sci.* 49:713–19

Guo H, Atchison DA, Birt BJ. 2008. Changes in through-focus spatial visual performance with adaptive optics correction of monochromatic aberrations. *Vis. Res.* 48:1804–11

Harmening WM, Tiruveedhula P, Roorda A, Sincich LC. 2012. Measurement and correction of transverse chromatic offsets for multi-wavelength retinal microscopy in the living eye. *Biomed. Opt. Express* 3:2066–77

Harmening WM, Tuten WS, Roorda A, Sincich LC. 2014. Mapping the perceptual grain of the human retina. *J. Neurosci.* 34:5667–77

Hauswirth WW, Aleman TS, Kaushal S, Cideciyan AV, Schwartz SB, et al. 2008. Treatment of Leber congenital amaurosis due to *RPE65* mutations by ocular subretinal injection of adeno-associated virus gene vector: short-term results of a phase I trial. *Hum. Gene Ther.* 19:979–90

Hirsch J, Curcio CA. 1989. The spatial resolution capacity of human foveal retina. *Vis. Res.* 29:1095–101

Hofer H, Carroll J, Neitz J, Neitz M, Williams DR. 2005a. Organization of the human trichromatic cone mosaic. *J. Neurosci.* 25:9669–79

Hofer H, Singer B, Williams DR. 2005b. Different sensations from cones with the same pigment. *J. Vis.* 5:444–54

Hofer H, Sredar N, Queener H, Li C, Porter J. 2011. Wavefront sensorless adaptive optics ophthalmoscopy in the human eye. *Opt. Express* 19:14160–71

Huang G, Gast TJ, Burns SA. 2014. In vivo adaptive optics imaging of the temporal raphe and its relationship to the optic disc and fovea in the human retina. *Investig. Ophthalmol. Vis. Sci.* 55:5952–61

Huang G, Qi X, Chui TYP, Zhong Z, Burns SA. 2012. A clinical planning module for adaptive optics SLO imaging. *Optom. Vis. Sci.* 89:593–601

Hunter JJ, Masella B, Dubra A, Sharma R, Yin L, et al. 2011. Images of photoreceptors in living primate eyes using adaptive optics two-photon ophthalmoscopy. *Biomed. Opt. Express* 2:139–48

Hunter JJ, Morgan JI, Merigan WH, Sliney DH, Sparrow JR, Williams DR. 2012. The susceptibility of the retina to photochemical damage from visible light. *Prog. Retin. Eye Res.* 31:28–42

Ivers KM, Li C, Patel N, Sredar N, Luo X, et al. 2011. Reproducibility of measuring lamina cribrosa pore geometry in human and nonhuman primates with in vivo adaptive optics imaging. *Investig. Ophthalmol. Vis. Sci.* 52:5473–80

Johnson PT, Lewis GP, Talaga KC, Brown MN, Kappel PJ, et al. 2003. Drusen-associated degeneration in the retina. *Investig. Ophthalmol. Vis. Sci.* 44:4481–88

Jonnal RS, Besecker JR, Derby JC, Kocaoglu OP, Cense B, et al. 2010. Imaging outer segment renewal in living human cone photoreceptors. *Opt. Express* 18:5257–70

Jonnal RS, Kocaoglu OP, Wang Q, Lee S, Miller DT. 2012. Phase-sensitive imaging of the outer retina using optical coherence tomography and adaptive optics. *Biomed. Opt. Express* 3:104–24

Jonnal RS, Kocaoglu OP, Zawadzki RJ, Lee SH, Werner JS, Miller DT. 2014. The cellular origins of the outer retinal bands in optical coherence tomography images. *Investig. Ophthalmol. Vis. Sci.* 55:7904–18

Kohl S, Varsanyi B, Antunes GA, Baumann B, Hoyng CB, et al. 2005. *CNGB3* mutations account for 50% of all cases with autosomal recessive achromatopsia. *Eur. J. Hum. Genet.* 13:302–8

Landa G, Gentile RC, Garcia PM, Muldoon TO, Rosen RB. 2012. External limiting membrane and visual outcome in macular hole repair: spectral domain OCT analysis. *Eye* 26:61–69

Larocca F, Dhalla AH, Kelly MP, Farsiu S, Izatt JA. 2013. Optimization of confocal scanning laser ophthalmoscope design. *J. Biomed. Opt.* 18:076015

Li KY, Mishra S, Tiruveedhula P, Roorda A. 2009. Comparison of control algorithms for a MEMS-based adaptive optics scanning laser ophthalmoscope. *Proc. Am. Control Conf., June 10–12, St. Louis, Mo.*, pp. 3848–53. Piscataway, NJ: IEEE

Li KY, Roorda A. 2007. Automated identification of cone photoreceptors in adaptive optics retinal images. *J. Opt. Soc. Am. A* 24:1358–63

Liang J, Grimm B, Goelz S, Bille JF. 1994. Objective measurement of wave aberrations of the human eye with use of a Hartmann–Shack wave-front sensor. *J. Opt. Soc. Am. A* 11:1949–57

Liang J, Williams DR. 1997. Aberrations and retinal image quality of the normal human eye. *J. Opt. Soc. Am. A* 14:2873–83

Liang J, Williams DR, Miller D. 1997. Supernormal vision and high-resolution retinal imaging through adaptive optics. *J. Opt. Soc. Am. A* 14:2884–92

Lim LS, Mitchell P, Seddon JM, Holz FG, Wong TY. 2012. Age-related macular degeneration. *Lancet* 379:1728–38

Lujan BJ, Roorda A, Knighton RW, Carroll J. 2011. Revealing Henle's fiber layer using spectral domain optical coherence tomography. *Investig. Ophthalmol. Vis. Sci.* 52:1486–92

Maguire AM, Simonelli F, Pierce EA, Pugh EN Jr, Mingozzi F, et al. 2008. Safety and efficacy of gene transfer for Leber's congenital amaurosis. *N. Engl. J. Med.* 358:2240–48

Makous W, Carroll J, Wolfing JI, Lin J, Christie N, Williams DR. 2006. Retinal microscotomas revealed with adaptive-optics microflashes. *Investig. Ophthalmol. Vis. Sci.* 47:4160–67

Martin JA, Roorda A. 2009. Pulsatility of parafoveal capillary leukocytes. *Exp. Eye Res.* 88:356–60

Masella BD, Hunter JJ, Williams DR. 2014a. New wrinkles in retinal densitometry. *Investig. Ophthalmol. Vis. Sci.* 55:7525–34

Masella BD, Hunter JJ, Williams DR. 2014b. Rod photopigment kinetics after photodisruption of the retinal pigment epithelium. *Investig. Ophthalmol. Vis. Sci.* 55:7535–44

Meadway A, Wang X, Curcio CA, Zhang Y. 2014. Microstructure of subretinal drusenoid deposits revealed by adaptive optics imaging. *Biomed. Opt. Express* 5:713–27

Milam AH, Li Z-Y, Fariss RN. 1998. Histopathology of the human retina in retinitis pigmentosa. *Prog. Retinal Eye Res.* 17:175–205

Miller DT, Roorda A. 2009. Adaptive optics in retinal microscopy and vision. In *Handbook of Optics* Vol III, ed. M Bass. Rochester, NY: Opt. Soc. Am.

Morgan JI, Dubra A, Wolfe R, Merigan WH, Williams DR. 2009. In vivo autofluorescence imaging of the human and macaque retinal pigment epithelial cell mosaic. *Investig. Ophthalmol. Vis. Sci.* 50:1350–59

Morgan JI, Hunter JJ, Masella B, Wolfe R, Gray DC, et al. 2008. Light-induced retinal changes observed with high-resolution autofluorescence imaging of the retinal pigment epithelium. *Investig. Ophthalmol. Vis. Sci.* 49:3715–29

Nadler Z, Wang B, Schuman JS, Ferguson RD, Patel A, et al. 2014. In vivo three-dimensional characterization of the healthy human lamina cribrosa with adaptive optics spectral-domain optical coherence tomography. *Investig. Ophthalmol. Vis. Sci.* 55:6459–66

Ooto S, Hangai M, Takayama K, Ueda-Arakawa N, Hanebuchi M, Yoshimura N. 2012. Photoreceptor damage and foveal sensitivity in surgically closed macular holes: an adaptive optics scanning laser ophthalmoscopy study. *Am. J. Ophthalmol.* 154:174–86

Ooto S, Hangai M, Takayama K, Ueda-Arakawa N, Tsujikawa A, et al. 2013. Comparison of cone pathologic changes in idiopathic macular telangiectasia types 1 and 2 using adaptive optics scanning laser ophthalmoscopy. *Am. J. Ophthalmol.* 155:1045–57

Ooto S, Hangai M, Yoshimura N. 2011. Photoreceptor restoration in unilateral acute idiopathic maculopathy on adaptive optics scanning laser ophthalmoscopy. *Arch. Ophthalmol.* 129:1633–35

Pinhas A, Dubow M, Shah N, Chui TY, Scoles D, et al. 2013. In vivo imaging of human retinal microvasculature using adaptive optics scanning light ophthalmoscope fluorescein angiography. *Biomed. Opt. Express* 4:1305–17

Popovic Z, Knutsson P, Thaung J, Owner-Petersen M, Sjostrand J. 2011. Noninvasive imaging of human foveal capillary network using dual-conjugate adaptive optics. *Investig. Ophthalmol. Vis. Sci.* 52:2649–55

Porter J. 2006. *Adaptive Optics for Vision Science*. Hoboken, NJ: Wiley-Interscience

Putnam NM, Hammer DX, Zhang Y, Merino D, Roorda A. 2010. Modeling the foveal cone mosaic imaged with adaptive optics scanning laser ophthalmoscopy. *Opt. Express* 18:24902–16

Putnam NM, Hofer H, Doble N, Chen L, Carroll J, Williams DR. 2005. The locus of fixation and the foveal cone mosaic. *J. Vis.* 5:632–39

Ramaswamy G, Lombardo M, Devaney N. 2014. Registration of adaptive optics corrected retinal nerve fiber layer (RNFL) images. *Biomed. Opt. Express* 5:1941–51

Rha J, Jonnal RS, Thorn KE, Qu J, Zhang Y, Miller DT. 2006. Adaptive optics flood-illumination camera for high speed retinal imaging. *Opt. Express* 14:4552–69

Rha J, Schroeder B, Godara P, Carroll J. 2009. Variable optical activation of human cone photoreceptors visualized using a short coherence light source. *Opt. Lett.* 34:3782–84

Rodieck RW. 1998. *The First Steps in Seeing*. Sunderland, MA: Sinauer Associates

Roorda A. 2011. Adaptive optics for studying visual function: a comprehensive review. *J. Vis.* 11(5):6

Roorda A, Romero-Borja F, Donnelly WJ, Queener H, Hebert TJ, Campbell MCW. 2002. Adaptive optics scanning laser ophthalmoscopy. *Opt. Express* 10:405–12

Roorda A, Williams DR. 1999. The arrangement of the three cone classes in the living human eye. *Nature* 397:520–22

Roorda A, Williams DR. 2002. Optical fiber properties of individual human cones. *J. Vis.* 2:404–12

Roorda A, Zhang Y, Duncan JL. 2007. High-resolution in vivo imaging of the RPE mosaic in eyes with retinal disease. *Investig. Ophthalmol. Vis. Sci.* 48:2297–303

Rossi EA, Rangel-Fonseca P, Parkins K, Fischer W, Latchney LR, et al. 2013. In vivo imaging of retinal pigment epithelium cells in age related macular degeneration. *Biomed. Opt. Express* 4:2527–39

Rossi EA, Roorda A. 2010. The relationship between visual resolution and cone spacing in the human fovea. *Nat. Neurosci.* 13:156–57

Sawides L, Gambra E, Pascual D, Dorronsoro C, Marcos S. 2010. Visual performance with real-life tasks under adaptive-optics ocular aberration correction. *J. Vis.* 10(5):19

Schallek J, Geng Y, Nguyen H, Williams DR. 2013. Morphology and topography of retinal pericytes in the living mouse retina using in vivo adaptive optics imaging and ex vivo characterization. *Investig. Ophthalmol. Vis. Sci.* 54:8237–50

Schwartz SD, Hubschman J-P, Heilwell G, Franco-Cardenas V, Pan CK, et al. 2012. Embryonic stem cell trials for macular degeneration: a preliminary report. *Lancet* 379:713–20

Schwartz SD, Regillo CD, Lam BL, Eliott D, Rosenfeld PJ, et al. 2015. Human embryonic stem cell-derived retinal pigment epithelium in patients with age-related macular degeneration and Stargardt's macular dystrophy: follow-up of two open-label phase 1/2 studies. *Lancet* 385:509–16

Schwarz C, Manzanera S, Artal P. 2014. Binocular visual performance with aberration correction as a function of light level. *J. Vis.* 14(14):6

Scoles D, Higgins BP, Cooper RF, Dubis AM, Summerfelt P, et al. 2014a. Microscopic inner retinal hyper-reflective phenotypes in retinal and neurologic disease. *Investig. Ophthalmol. Vis. Sci.* 55:4015–29

Scoles D, Sulai YN, Dubra A. 2013. In vivo dark-field imaging of the retinal pigment epithelium cell mosaic. *Biomed. Opt. Express* 4:1710–23

Scoles D, Sulai YN, Langlo CS, Fishman GA, Curcio CA, et al. 2014b. In vivo imaging of human cone photoreceptor inner segments. *Investig. Ophthalmol. Vis. Sci.* 55:4244–51

Sharma R, Yin L, Geng Y, Merigan WH, Palczewska G, et al. 2013. In vivo two-photon imaging of the mouse retina. *Biomed. Opt. Express* 4:1285–93

Sredar N, Ivers KM, Queener HM, Zouridakis G, Porter J. 2013. 3D modeling to characterize lamina cribrosa surface and pore geometries using in vivo images from normal and glaucomatous eyes. *Biomed. Opt. Express* 4:1153–65

Stevenson SB, Roorda A. 2005. Correcting for miniature eye movements in high resolution scanning laser ophthalmoscopy. In *Ophthalmic Technologies XI*, ed. F Manns, P Soderberg, A Ho, pp. 145–51. Bellingham, WA: SPIE

Sulai YN, Dubra A. 2014. Non-common path aberration correction in an adaptive optics scanning ophthalmoscope. *Biomed. Opt. Express* 5:3059–73

Sulai YN, Scoles D, Harvey Z, Dubra A. 2014. Visualization of retinal vascular structure and perfusion with a nonconfocal adaptive optics scanning light ophthalmoscope. *J. Opt. Soc. Am. A* 31:569–79

Sundaram V, Wilde C, Aboshiha J, Cowing J, Han C, et al. 2014. Retinal structure and function in achromatopsia: implications for gene therapy. *Ophthalmology* 121:234–45

Takayama K, Ooto S, Hangai M, Arakawa N, Oshima S, et al. 2012. High-resolution imaging of the retinal nerve fiber layer in normal eyes using adaptive optics scanning laser ophthalmoscopy. *PLOS ONE* 7:e33158

Talcott KE, Ratnam K, Sundquist SM, Lucero AS, Lujan BJ, et al. 2011. Longitudinal study of cone photoreceptors during retinal degeneration and in response to ciliary neurotrophic factor treatment. *Investig. Ophthalmol. Vis. Sci.* 52:2219–26

Tam J, Dhamdhere KP, Tiruveedhula P, Manzanera S, Barez S, et al. 2011a. Disruption of the retinal parafoveal capillary network in type 2 diabetes before the onset of diabetic retinopathy. *Investig. Ophthalmol. Vis. Sci.* 52:9257–66

Tam J, Tiruveedhula P, Roorda A. 2011b. Characterization of single-file flow through human retinal parafoveal capillaries using an adaptive optics scanning laser ophthalmoscope. *Biomed. Opt. Express* 2:781–93

Tuten WS, Tiruveedhula P, Roorda A. 2012. Adaptive optics scanning laser ophthalmoscope-based microperimetry. *Optom. Vis. Sci.* 89:563–74

Vienola KV, Braaf B, Sheehy CK, Yang Q, Tiruveedhula P, et al. 2012. Real-time eye motion compensation for OCT imaging with tracking SLO. *Biomed. Opt. Express* 3:2950–63

Vilupuru AS, Rangaswamy NV, Frishman LJ, Smith EL III, Harwerth RS, Roorda A. 2007. Adaptive optics scanning laser ophthalmoscopy for in vivo imaging of lamina cribrosa. *J. Opt. Soc. Am. A* 24:1417–25

Wang Q, Tuten WS, Lujan BJ, Holland J, Bernstein PS, et al. 2015. Adaptive optics microperimetry and OCT images show preserved function and recovery of cone visibility in macular telangiectasia type 2 retinal lesions. *Investig. Ophthalmol. Vis. Sci.* 56:778–86

Webb RH, Hughes GW, Pomerantzeff O. 1980. Flying spot TV ophthalmoscope. *Appl. Opt.* 19:2991–97

Weiland JD, Cho AK, Humayun MS. 2011. Retinal prostheses: current clinical results and future needs. *Ophthalmology* 118:2227–37

Williams DR. 2011. Imaging single cells in the living retina. *Vis. Res.* 51:1379–96

Xue B, Choi SS, Doble N, Werner JS. 2007. Photoreceptor counting and montaging of en-face retinal images from an adaptive optics fundus camera. *J. Opt. Soc. Am. A* 24:1364–72

Yang Q, Arathorn DW, Tiruveedhula P, Vogel CR, Roorda A. 2010. Design of an integrated hardware interface for AOSLO image capture and cone-targeted stimulus delivery. *Opt. Express* 18:17841–58

Yannuzzi LA, Bardal AM, Freund KB, Chen K-J, Eandi CM, Blodi B. 2006. Idiopathic macular telangiectasia. *Arch. Ophthalmol.* 124:450–60

Yin L, Geng Y, Osakada F, Sharma R, Cetin AH, et al. 2013. Imaging light responses of retinal ganglion cells in the living mouse eye. *J. Neurophysiol.* 109:2415–21

Yin L, Masella B, Dalkara D, Zhang J, Flannery JG, et al. 2014. Imaging light responses of foveal ganglion cells in the living macaque eye. *J. Neurosci.* 34:6596–605

Yoon GY, Williams DR. 2002. Visual performance after correcting the monochromatic and chromatic aberrations of the eye. *J. Opt. Soc. Am. A* 19:266–75

Zawadzki RJ, Capps AG, Kim DY, Panorgias A, Stevenson SB, et al. 2014. Progress on developing adaptive optics–optical coherence tomography for retinal imaging: monitoring and correction of eye motion artifacts. *IEEE J. Sel. Top. Quantum Electron.* 20:7100912

Zawadzki RJ, Choi SS, Fuller AR, Evans JW, Hamann B, Werner JS. 2009. Cellular resolution volumetric in vivo retinal imaging with adaptive optics-optical coherence tomography. *Opt. Express* 17:4084–94

Zayit-Soudry S, Duncan JL, Syed R, Menghini M, Roorda AJ. 2013. Cone structure imaged with adaptive optics scanning laser ophthalmoscopy in eyes with nonneovascular age-related macular degeneration. *Investig. Ophthalmol. Vis. Sci.* 54:7498–509

Zhang Y, Poonja S, Roorda A. 2006. MEMS-based adaptive optics scanning laser ophthalmoscope. *Opt. Lett.* 31:1268–70

Zhang Y, Wang X, Rivero EB, Clark ME, Witherspoon CD, et al. 2014. Photoreceptor perturbation around subretinal drusenoid deposits as revealed by adaptive optics scanning laser ophthalmoscopy. *Am. J. Ophthalmol.* 158:584–96

Zhong Z, Song H, Chui TYP, Petrig BL, Burns SA. 2011. Noninvasive measurements and analysis of blood velocity profiles in human retinal vessels. *Investig. Ophthalmol. Vis. Sci.* 52:4151–57
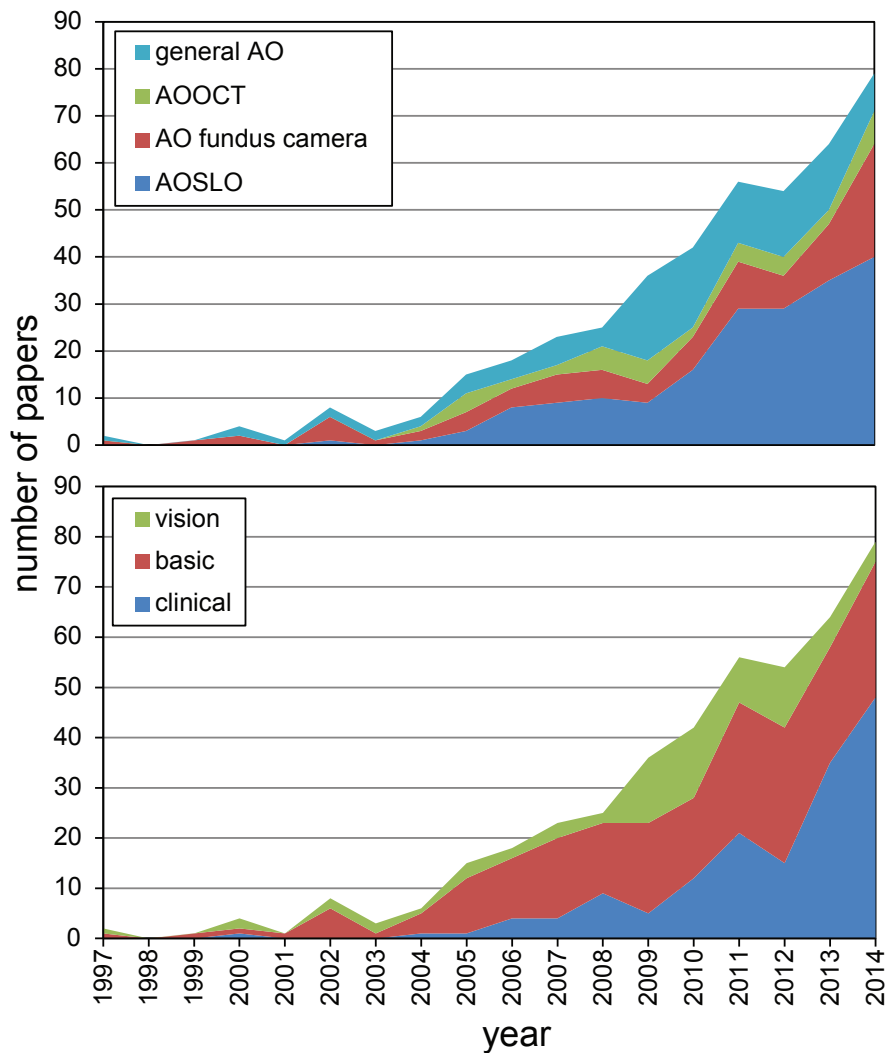
Contents

Errata

An online log of corrections to *Annual Review of Vision Science* articles may be found at
http://www.annualreviews.org/errata/vision

Supplemental Figure 1: These charts plot eye and vision related AO papers published to the end of 2014. General AO papers are those whose results are generally applicable to any AO modality (e.g.: use of woofer tweeter deformable mirrors to optimize AO correction). Papers reporting combined technologies (e.g. AOSLO and AOOCT were divided equally between their respective categories. Clinical science papers were defined as those that report AO retinal images or AO data acquired from patients with disease. Basic science papers are those that report a new AO-based technology, a new imaging target, a novel AO image analysis, or report on a basic property of retinal structure or physiology (e.g. mapping of the trichromatic cone mosaic). Vision applications include those studies that use AO to study how optics and blur affect vision, but do not involve retinal imaging in any form.

Supplemental Table 1: AO clinical publications tabulated by disease and retinal location imaged

Inner Retinal Disease and Neuropathies

  Glaucoma:

  Nerve fiber layer: (Chen et al 2015, Scoles et al 2014a, Takayama et al 2012)

  Lamina cribrosa: (Akagi et al 2012, Lombardo et al 2013c, Sredar et al 2013)

  Cones: (Choi et al 2008, Werner et al 2011)

  Epiretinal membrane: (Lombardo et al 2013b, Ooto et al 2011b, Scoles et al 2014a)

  Gunn's dots: (Paques et al 2015, Scoles et al 2014a)

  Optic nerve drusen with non arteric ischemic optic neuropathy (cone imaging): (Choi et al 2008, Scoles et al 2014a)

  Optic atrophy: (Gocho et al 2013a, Scoles et al 2014a)

  Optic neuritis: (Scoles et al 2014a)

  Multiple sclerosis: (Scoles et al 2014a)

  Parkinson's disease: (Scoles et al 2014a)

Retinal Vasculature Disease

  Diabetes

  Vasculature: (Arichika et al 2014a, Burns et al 2014, Chui et al 2014, Deak & Schmidt-Erfurth 2013, Dubow et al 2014, Lombardo et al 2013a, Pinhas et al 2014, Scoles et al 2014a, Stepushina & Bol'shunov 2011, Tam et al 2012, Tam et al 2011)

  Hard exudates: (Burns et al 2014, Roorda et al 2006)

  Cones: (Lombardo et al 2014, Tam et al 2012)

  Hypertension: (Arichika et al 2014b, Chui et al 2014, Koch et al 2014, Pinhas et al 2014, Stepushina & Bol'shunov 2011)

  Branch retinal vein occlusion: (Akagi-Kurashige et al 2014, Chui et al 2014, Scoles et al 2014a)

  Central vein occlusion: (Chui et al 2014)

  Central macular arteriovenous malformation: (Telander et al 2010)

  Retinal vasculitis: (Errera et al 2014)

  Hyperlipidemia: (Pinhas et al 2014)

  Sickle cell disease: (Pinhas et al 2014)

Ocular Toxicity and Trauma

  Ocular siderosis: (Faure et al 2014)

  Hydroxychloroquine retinal toxicity: (Jacob et al 2015, Stepien et al 2009)

  Chloroquine maculopathy: (Bae et al 2014)

  Response to surgeries

  Laser photocoagulation for hemiretinal vein occlusion and proliferative diabetic retinopathy: (Han et al 2012)

  Macular translocation for AMD: (Muthiah et al 2014)

  Retinal detachment surgery: (Saleh et al 2014)

  Ocular trauma

  Blunt force: (Flatter et al 2014, Langlo et al 2014, Stepien et al 2012)

  Solar retinopathy: (Roorda et al 2006)

  Laser injury: (Kitaguchi et al 2009)

  Macular holes: (Debellemaniere et al 2014, Hansen et al 2015, Kitaguchi et al 2008, Ooto et al 2012, Ooto et al 2014, Scoles et al 2014a, Yokota et al 2013)

Outer retinal disease (not including inherited retinal degenerations with known gene mutations)

Age-related macular degeneration (AMD)

Photoreceptors and/or drusen: (Boretsky et al 2012, Godara et al 2010c, Land et al 2014, Meadway et al 2014, Mrejen et al 2014b, Obata & Yanagi 2014, Querques et al 2014, Querques et al 2012, Zayit-Soudry et al 2013, Zhang et al 2014)

Retinal pigment epithelium: (Rossi et al 2013b)

Geographic atrophy: (Gocho et al 2013b, Zayit-Soudry et al 2013)

Inner retina: (Scoles et al 2014a)

Macular telangiectasia type 2: (Jacob et al 2015, Massamba et al 2011, Ooto et al 2011a, Ooto et al 2013, Scoles et al 2014a, Wang et al 2015)

Albinism: (Godara et al 2010a, Marmor et al 2008, McAllister et al 2010, Wilk et al 2014)

Central serous chorioretinopathy: (Ooto et al 2010, Scoles et al 2014a)

Birdshot choroidoretinopathy: (Scoles et al 2014a)

Rubella retinopathy: (Scoles et al 2014a)

Inflammatory retinopathies

AZOOR: (Merino et al 2011, Mkrtchyan et al 2012, Nakao et al 2014)

Acute macular neuroretinopathy: (Garnier et al 2015, Hansen et al 2013, Mrejen et al 2014a)

Acute posterior multifocal placoid pigment epitheliopathy: (Hong et al 2014, Jacob et al 2015, Mrejen et al 2013)

Unilateral acute idiopathic maculopathy: (Ooto et al 2011c)

Multiple evanescent white dot syndrome: (Boretsky et al 2013)

Other maculopathies

Bilateral maculopathy: (Godara et al 2010b)

Central ring scotoma: (Joeres et al 2008)

Bull's eye maculopathy: (Bessho et al 2008)

Inherited retinal degenerations

RHO (autosomal dominant retinitis pigmentosa): (Choi et al 2006, Duncan et al 2007, Menghini et al 2015, Park et al 2014)

CNBA3 ,CNGB3, GNAT2, PDE6C (achromatopsia): (Carroll et al 2008, Dubis et al 2014, Genead et al 2011, Merino et al 2011, Scoles et al 2014b, Sundaram et al 2014, Vincent et al 2013b)

OPN1LW/OPN1MW /OPN1SW

(blue cone monochromacy): (Carroll et al 2010, Cideciyan et al 2013, Rossi et al 2013a)

(red-green color vision defects): (Carroll et al 2009, Carroll et al 2012, Carroll et al 2004, Makous et al 2006, McClements et al 2013, Rha et al 2010, Wagner-Schuman et al 2010)

(tritan defects): (Baraas et al 2007)

REP1 (Choroideremia): (Morgan et al 2014, Scoles et al 2014a, Syed et al 2013)

RS1 (X-linked retinoschisis): (Duncan et al 2011a)

CLRN1 (Ushers type III): (Ratnam et al 2013)

CDHR1 (autosomal recessive retinal degeneration): (Duncan et al 2012)

FAM161A (autosomal recessive retinal degeneration): (Duncan et al 2014)

SNRNP200 (autosomal dominant retinitis pigmentosa): (Bowne et al 2013)

CYP4V2 (Bietti crystalline dystrophy): (Gocho et al 2014)

NR2E3 (enhanced S-cone syndrome): (Park et al 2013)

KCNV2 (cone dystrophy): (Vincent et al 2013a)

GRM6 (congenital stationary night blindness): (Godara et al 2012)
GRK1 (Oguchi disease): (Godara et al 2012)
Peripherin/RDS (retinal degeneration): (Duncan et al 2011b)
RLBP1 (retinitis punctata albescens): (Dessalces et al 2013)
RDH5 (fundus albipunctatus): (Makiyama et al 2014, Song et al 2014)
Mitochondrial DNA *T8993C* (NARP): (Gelfand et al 2011, Yoon et al 2009)
ABCA4 (Stargardt's disease): (Chen et al 2011, Pang et al 2015, Scoles et al 2014a, Xue et al 2007)
BEST1 (Best's vitelliform dystrophy): (Kay et al 2013, Scoles et al 2014a)
RPGR (cone rod dystrophy) (Duncan et al 2007)
RPGR (X-linked retinitis pigmentosa): (Menghini et al 2015)
ABCA4 (autosomal recessive retinitis pigmentosa): (Menghini et al 2015)
RPGR and RP2 (female carriers of XLRP): (Pyo et al 2013)
CEP290 (Leber's congenital amaurosis): (Scoles et al 2014a)
Cone-rod dystrophy: (Choi et al 2006, Duncan et al 2007, Scoles et al 2014a, Wolfing et al 2006)
Rod-cone dystrophy: (Choi et al 2006)
Occult macular dystrophy: (Kitaguchi et al 2011, Tojo et al 2013)
Oligocone trichromacy: (Michaelides et al 2011)

Akagi-Kurashige Y, Tsujikawa A, Ooto S, Makiyama Y, Muraoka Y, et al. 2014. Retinal microstructural changes in eyes with resolved branch retinal vein occlusion: an adaptive optics scanning laser ophthalmoscopy study. *American Journal of Ophthalmology* 157: 1239-49

Akagi T, Hangai M, Takayama K, Nonaka A, Ooto S, Yoshimura N. 2012. In vivo imaging of lamina cribrosa pores by adaptive optics scanning laser ophthalmoscopy. *Invest Ophthalmol.Vis.Sci.* 53: 4111-19

Arichika S, Uji A, Murakami T, Unoki N, Yoshitake S, et al. 2014a. Retinal hemorheologic characterization of early-stage diabetic retinopathy using adaptive optics scanning laser ophthalmoscopy. *Invest Ophthalmol Vis Sci* 55: 8513-22

Arichika S, Uji A, Yoshimura N. 2014b. Adaptive optics assisted visualization of thickened retinal arterial wall in a patient with controlled malignant hypertension. *Clinical ophthalmology* 8: 2041-3

Bae EJ, Kim KR, Tsang SH, Park SP, Chang S. 2014. Retinal damage in chloroquine maculopathy, revealed by high resolution imaging: a case report utilizing adaptive optics scanning laser ophthalmoscopy. *Korean J.Ophthalmol.* 28: 100-07

Baraas RC, Carroll J, Gunther KL, Chung M, Williams DR, et al. 2007. Adaptive optics retinal imaging reveals S-cone dystrophy in tritan color-vision deficiency. *J.Opt.Soc.Am.A Opt.Image Sci.Vis.* 24: 1438-47

Bessho K, Fujikado T, Mihashi T, Yamaguchi T, Nakazawa N, Tano Y. 2008. Photoreceptor images of normal eyes and of eyes with macular dystrophy obtained in vivo with an adaptive optics fundus camera. *Jpn.J.Ophthalmol.* 52: 380-85

Boretsky A, Khan F, Burnett G, Hammer DX, Ferguson RD, et al. 2012. In vivo imaging of photoreceptor disruption associated with age-related macular degeneration: A pilot study. *Lasers Surg.Med.* 44: 603-10

Boretsky A, Mirza S, Khan F, Motamedi M, van Kuijk FJ. 2013. High-resolution multimodal imaging of multiple evanescent white dot syndrome. *Ophthalmic Surg.Lasers Imaging Retina* 44: 296-300

Bowne SJ, Sullivan LS, Avery CE, Sasser EM, Roorda A, et al. 2013. Mutations in the small nuclear riboprotein 200 kDa gene (SNRNP200) cause 1.6% of autosomal dominant retinitis pigmentosa. *Molecular Vision* 19 2407-17

Burns SA, Elsner AE, Chui TY, Vannasdale DA, Jr., Clark CA, et al. 2014. In vivo adaptive optics microvascular imaging in diabetic patients without clinically severe diabetic retinopathy. *Biomed.Opt.Express* 5: 961-74

Carroll J, Baraas RC, Wagner-Schuman M, Rha J, Siebe CA, et al. 2009. Cone photoreceptor mosaic disruption associated with Cys203Arg mutation in the M-cone opsin. *Proc.Natl.Acad.Sci.U.S.A* 106: 20948-53

Carroll J, Choi SS, Williams DR. 2008. In vivo imaging of the photoreceptor mosaic of a rod monochromat. *Vision Research* 48: 2564-68

Carroll J, Dubra A, Gardner JC, Mizrahi-Meissonnier L, Cooper RF, et al. 2012. The effect of cone opsin mutations on retinal structure and the integrity of the photoreceptor mosaic. *Invest Ophthalmol.Vis.Sci.* 53: 8006-15

Carroll J, Neitz M, Hofer H, Neitz J, Williams DR. 2004. Functional photoreceptor loss revealed with adaptive optics: an alternate cause of color blindness. *Proc.Natl.Acad.Sci.U.S.A* 101: 8461-66

Carroll J, Rossi EA, Porter J, Neitz J, Roorda A, et al. 2010. Deletion of the X-linked opsin gene array locus control region (LCR) results in disruption of the cone mosaic. *Vision Research* 50: 1989-99

Chen MF, Chui TY, Alhadeff P, Rosen RB, Ritch R, et al. 2015. Adaptive optics imaging of healthy and abnormal regions of retinal nerve fiber bundles of patients with glaucoma. *Invest Ophthalmol Vis Sci* 56: 674-81

Chen Y, Ratnam K, Sundquist SM, Lujan B, Ayyagari R, et al. 2011. Cone photoreceptor abnormalities correlate with vision loss in patients with Stargardt disease. *Invest Ophthalmol.Vis.Sci.* 52: 3281-92

Choi SS, Doble N, Hardy JL, Jones SM, Keltner JL, et al. 2006. In vivo imaging of the photoreceptor mosaic in retinal dystrophies and correlations with visual function. *Invest Ophthalmol.Vis.Sci.* 47: 2080-92

Choi SS, Zawadzki RJ, Keltner JL, Werner JS. 2008. Changes in cellular structures revealed by ultra-high resolution retinal imaging in optic neuropathies. *Invest Ophthalmol.Vis.Sci.* 49: 2103-19

Chui TY, Dubow M, Pinhas A, Shah N, Gan A, et al. 2014. Comparison of adaptive optics scanning light ophthalmoscopic fluorescein angiography and offset pinhole imaging. *Biomed.Opt.Express* 5: 1173-89

Cideciyan AV, Hufnagel RB, Carroll J, Sumaroka A, Luo X, et al. 2013. Human cone visual pigment deletions spare sufficient photoreceptors to warrant gene therapy. *Hum.Gene Ther.* 24: 993-1006

Deak GG, Schmidt-Erfurth U. 2013. Imaging of the parafoveal capillary network in diabetes. *Curr.Diab.Rep.* 13: 469-75

Debellemaniere G, Koehl A, Delbosc B, Saleh M. 2014. [High-resolution retinal imaging using adaptive optics of a full thickness macular hole]. *Journal francais d'ophtalmologie* 37: 502-3

Dessalces E, Bocquet B, Bourien J, Zanlonghi X, Verdet R, et al. 2013. Early-onset foveal involvement in retinitis punctata albescens with mutations in RLBP1. *JAMA Ophthalmol.* 131: 1314-23

Dubis AM, Cooper RF, Aboshiha J, Langlo CS, Sundaram V, et al. 2014. Genotype-dependent variability in residual cone structure in achromatopsia: toward developing metrics for assessing cone health. *Invest Ophthalmol Vis Sci* 55: 7303-11

Dubow M, Pinhas A, Shah N, Cooper RF, Gan A, et al. 2014. Classification of human retinal microaneurysms using adaptive optics scanning light ophthalmoscope fluorescein angiography. *Invest Ophthalmol.Vis.Sci.* 55: 1299-309

Duncan JL, Biswas P, Kozak I, Navani M, Syed R, et al. 2014. Ocular Phenotype of a Family with FAM161A-associated Retinal Degeneration. *Ophthalmic Genet.*: 1-9

Duncan JL, Ratnam K, Birch DG, Sundquist SM, Lucero AS, et al. 2011a. Abnormal cone structure in foveal schisis cavities in X-linked retinoschisis from mutations in exon 6 of the RS1 gene. *Invest Ophthalmol.Vis.Sci.* 52: 9614-23

Duncan JL, Roorda A, Navani M, Vishweswaraiah S, Syed R, et al. 2012. Identification of a Novel Mutation in the CDHR1 Gene in a Family With Recessive Retinal Degeneration. *Archives of Ophthalmology* 130: 1301-08

Duncan JL, Talcott KE, Ratnam K, Sundquist SM, Lucero AS, et al. 2011b. Cone Structure in Retinal Degeneration Associated with Mutations in the peripherin/RDS Gene. *Invest Ophthalmol.Vis.Sci.* 52: 1557-66

Duncan JL, Zhang Y, Gandhi J, Nakanishi C, Othman M, et al. 2007. High-resolution imaging with adaptive optics in patients with inherited retinal degeneration. *Invest Ophthalmol.Vis.Sci.* 48: 3283-91

Errera MH, Coisy S, Fardeau C, Sahel JA, Kallel S, et al. 2014. Retinal vasculitis imaging by adaptive optics. *Ophthalmology* 121: 1311-12

Faure C, Gocho K, Le Mer Y, Sahel JA, Paques M, Audo I. 2014. Functional and high resolution retinal imaging assessment in a case of ocular siderosis. *Documenta Ophthalmologica* 128: 69-75

Flatter JA, Cooper RF, Dubow MJ, Pinhas A, Singh RS, et al. 2014. Outer retinal structure after closed-globe blunt ocular trauma. *Retina* 34: 2133-46

Garnier MB, Castelbou M, Tumahai P, Montard M, Delbosc B, Saleh M. 2015. [Acute macular neuroretinopathy and adaptive optics imaging. A case report.]. *Journal francais d'ophtalmologie*: [Epub ahead of print]

Gelfand JM, Duncan JL, Racine CA, Gillum LA, Chin CT, et al. 2011. Heterogeneous patterns of tissue injury in NARP syndrome. *Journal of neurology* 258: 440-8

Genead MA, Fishman GA, Rha J, Dubis AM, Bonci DM, et al. 2011. Photoreceptor structure and function in patients with congenital achromatopsia. *Invest Ophthalmol.Vis.Sci.* 52: 7298-308

Gocho K, Kameya S, Akeo K, Kikuchi S, Usui A, et al. 2014. High-Resolution Imaging of Patients with Bietti Crystalline Dystrophy with CYP4V2 Mutation. *J.Ophthalmol.* 2014: 283603

Gocho K, Kikuchi S, Kabuto T, Kameya S, Shinoda K, et al. 2013a. High-resolution en face images of microcystic macular edema in patients with autosomal dominant optic atrophy. *Biomed.Res.Int.* 2013: 676803

Gocho K, Sarda V, Falah S, Sahel JA, Sennlaub F, et al. 2013b. Adaptive optics imaging of geographic atrophy. *Invest Ophthalmol.Vis.Sci.* 54: 3673-80

Godara P, Cooper RF, Sergouniotis PI, Diederichs MA, Streb MR, et al. 2012. Assessing retinal structure in complete congenital stationary night blindness and Oguchi disease. *American Journal of Ophthalmology* 154: 987-1001

Godara P, Dubis AM, Roorda A, Duncan JL, Carroll J. 2010a. Adaptive optics retinal imaging: emerging clinical applications. *Optometry and Vision Science* 87: 930-41

Godara P, Rha J, Tait DM, McAllister J, Dubis A, et al. 2010b. Unusual adaptive optics findings in a patient with bilateral maculopathy. *Archives of Ophthalmology* 128: 253-54

Godara P, Siebe C, Rha J, Michaelides M, Carroll J. 2010c. Assessing the photoreceptor mosaic over drusen using adaptive optics and SD-OCT. *Ophthalmic Surg.Lasers Imaging* 41 Suppl: S104-S08

Han DP, Croskrey JA, Dubis AM, Schroeder B, Rha J, Carroll J. 2012. Adaptive optics and spectral-domain optical coherence tomography of human photoreceptor structure after short-duration [corrected] pascal macular grid and panretinal laser photocoagulation. *Archives of Ophthalmology* 130: 518-21

Hansen S, Batson S, Weinlander KM, Cooper RF, Scoles DH, et al. 2015. Assessing photoreceptor structure after macular hole closure. *Retinal cases & brief reports* 9: 15-20

Hansen SO, Cooper RF, Dubra A, Carroll J, Weinberg DV. 2013. Selective cone photoreceptor injury in acute macular neuroretinopathy. *Retina* 33: 1650-58

Hong IH, Park SP, Chen CL, Kim HK, Tsang SH, Chang S. 2014. Cone photoreceptor abnormalities correlate with vision loss in a case of acute posterior multifocal placoid pigment epitheliopathy. *Ophthalmic Surg.Lasers Imaging Retina* 45: 74-78

Jacob J, Paques M, Krivosic V, Dupas B, Couturier A, et al. 2015. Meaning of visualizing retinal cone mosaic on adaptive optics images. *Am J Ophthalmol* 159: 118-23 e1

Joeres S, Jones SM, Chen DC, Silva D, Olivier S, et al. 2008. Retinal imaging with adaptive optics scanning laser ophthalmoscopy in unexplained central ring scotoma. *Archives of Ophthalmology* 126: 543-47

Kay DB, Land ME, Cooper RF, Dubis AM, Godara P, et al. 2013. Outer retinal structure in best vitelliform macular dystrophy. *JAMA Ophthalmol.* 131: 1207-15

Kitaguchi Y, Fujikado T, Bessho K, Sakaguchi H, Gomi F, et al. 2008. Adaptive optics fundus camera to examine localized changes in the photoreceptor layer of the fovea. *Ophthalmology* 115: 1771-77

Kitaguchi Y, Fujikado T, Kusaka S, Yamaguchi T, Mihashi T, Tano Y. 2009. Imaging of titanium:sapphire laser retinal injury by adaptive optics fundus imaging and Fourier-domain optical coherence tomography. *American Journal of Ophthalmology* 148: 97-104

Kitaguchi Y, Kusaka S, Yamaguchi T, Mihashi T, Fujikado T. 2011. Detection of photoreceptor disruption by adaptive optics fundus imaging and Fourier-domain optical coherence tomography in eyes with occult macular dystrophy. *Clin.Ophthalmol.* 5: 345-51

Koch E, Rosenbaum D, Brolly A, Sahel JA, Chaumet-Riffaud P, et al. 2014. Morphometric analysis of small arteries in the human retina using adaptive optics imaging: relationship with blood pressure and focal vascular changes. *J.Hypertens.* 32: 890-98

Land ME, Cooper RF, Young J, Berg E, Kitchner T, et al. 2014. Cone Structure in Subjects with Known Genetic Relative Risk for AMD. *Optometry and Vision Science* 91: 939-49

Langlo CS, Flatter JA, Dubra A, Wirostko WJ, Carroll J. 2014. A lensing effect of inner retinal cysts on images of the photoreceptor mosaic. *Retina* 34: 421-22

Lombardo M, Parravano M, Lombardo G, Varano M, Boccassini B, et al. 2014. Adaptive optics imaging of parafoveal cones in type 1 diabetes. *Retina* 34: 546-57

Lombardo M, Parravano M, Serrao S, Ducoli P, Stirpe M, Lombardo G. 2013a. Analysis of retinal capillaries in patients with type 1 diabetes and nonproliferative diabetic retinopathy using adaptive optics imaging. *Retina* 33: 1630-39

Lombardo M, Scarinci F, Ripandelli G, Cupo G, Stirpe M, Serrao S. 2013b. Adaptive optics imaging of idiopathic epiretinal membranes. *Ophthalmology* 120: 1508-09

Lombardo M, Serrao S, Devaney N, Parravano M, Lombardo G. 2013c. Adaptive optics technology for high-resolution retinal imaging. *Sensors.(Basel)* 13: 334-66

Makiyama Y, Ooto S, Hangai M, Ogino K, Gotoh N, et al. 2014. Cone abnormalities in fundus albipunctatus associated with RDH5 mutations assessed using adaptive optics scanning laser ophthalmoscopy. *American Journal of Ophthalmology* 157: 558-70

Makous W, Carroll J, Wolfing JI, Lin J, Christie N, Williams DR. 2006. Retinal microscotomas revealed with adaptive-optics microflashes. *Invest Ophthalmol.Vis.Sci.* 47: 4160-67

Marmor MF, Choi SS, Zawadzki RJ, Werner JS. 2008. Visual insignificance of the foveal pit: reassessment of foveal hypoplasia as fovea plana. *Archives of Ophthalmology* 126: 907-13

Massamba N, Querques G, Lamory B, Querques L, Souied E, Soubrane G. 2011. In vivo evaluation of photoreceptor mosaic in type 2 idiopathic macular telangiectasia using adaptive optics. *Acta Ophthalmol.* 89: e601-e03

McAllister JT, Dubis AM, Tait DM, Ostler S, Rha J, et al. 2010. Arrested development: high-resolution imaging of foveal morphology in albinism. *Vision Research* 50: 810-17

McClements M, Davies WI, Michaelides M, Carroll J, Rha J, et al. 2013. X-linked cone dystrophy and colour vision deficiency arising from a missense mutation in a hybrid L/M cone opsin gene. *Vision Res* 80: 41-50

Meadway A, Wang X, Curcio CA, Zhang Y. 2014. Microstructure of subretinal drusenoid deposits revealed by adaptive optics imaging. *Biomed.Opt.Express* 5: 713-27

Menghini M, Lujan BJ, Zayit-Soudry S, Syed R, Porco TC, et al. 2015. Correlation of outer nuclear layer thickness with cone density values in patients with retinitis pigmentosa and healthy subjects. *Invest Ophthalmol.Vis.Sci.* 56: 372-81

Merino D, Duncan JL, Tiruveedhula P, Roorda A. 2011. Observation of cone and rod photoreceptors in normal subjects and patients using a new generation adaptive optics scanning laser ophthalmoscope. *Biomed.Opt.Express* 2: 2189-201

Michaelides M, Rha J, Dees EW, Baraas RC, Wagner-Schuman ML, et al. 2011. Integrity of the cone photoreceptor mosaic in oligocone trichromacy. *Invest Ophthalmol.Vis.Sci.* 52: 4757-64

Mkrtchyan M, Lujan BJ, Merino D, Thirkill CE, Roorda A, Duncan JL. 2012. Outer retinal structure in patients with acute zonal occult outer retinopathy. *American Journal of Ophthalmology* 153: 757-68, 68

Morgan JI, Han G, Klinman E, Maguire WM, Chung DC, et al. 2014. High-resolution adaptive optics retinal imaging of cellular structure in choroideremia. *Invest Ophthalmol.Vis.Sci.* 55: 6381-97

Mrejen S, Gallego-Pinazo R, Wald KJ, Freund KB. 2013. Acute posterior multifocal placoid pigment epitheliopathy as a choroidopathy: what we learned from adaptive optics imaging. *JAMA Ophthalmol.* 131: 1363-64

Mrejen S, Pang CE, Sarraf D, Goldberg NR, Gallego-Pinazo R, et al. 2014a. Adaptive optics imaging of cone mosaic abnormalities in acute macular neuroretinopathy. *Ophthalmic surgery, lasers & imaging retina* 45: 562-9

Mrejen S, Sato T, Curcio CA, Spaide RF. 2014b. Assessing the cone photoreceptor mosaic in eyes with pseudodrusen and soft Drusen in vivo using adaptive optics imaging. *Ophthalmology* 121: 545-51

Muthiah MN, Keane PA, Zhong J, Gias C, Uppal G, et al. 2014. Adaptive optics imaging shows rescue of macula cone photoreceptors. *Ophthalmology* 121: 430-31

Nakao S, Kaizu Y, Yoshida S, Iida T, Ishibashi T. 2014. Spontaneous remission of acute zonal occult outer retinopathy: follow-up using adaptive optics scanning laser ophthalmoscopy. *Graefes Arch.Clin.Exp.Ophthalmol.*: [Epub ahead of print]

Obata R, Yanagi Y. 2014. Quantitative analysis of cone photoreceptor distribution and its relationship with axial length, age, and early age-related macular degeneration. *PLoS One* 9: e91873

Ooto S, Hangai M, Sakamoto A, Tsujikawa A, Yamashiro K, et al. 2010. High-resolution imaging of resolved central serous chorioretinopathy using adaptive optics scanning laser ophthalmoscopy. *Ophthalmology* 117: 1800-9, 09

Ooto S, Hangai M, Takayama K, Arakawa N, Tsujikawa A, et al. 2011a. High-resolution photoreceptor imaging in idiopathic macular telangiectasia type 2 using adaptive optics scanning laser ophthalmoscopy. *Invest Ophthalmol.Vis.Sci.* 52: 5541-50

Ooto S, Hangai M, Takayama K, Sakamoto A, Tsujikawa A, et al. 2011b. High-resolution imaging of the photoreceptor layer in epiretinal membrane using adaptive optics scanning laser ophthalmoscopy. *Ophthalmology* 118: 873-81

Ooto S, Hangai M, Takayama K, Ueda-Arakawa N, Hanebuchi M, Yoshimura N. 2012. Photoreceptor damage and foveal sensitivity in surgically closed macular holes: an adaptive optics scanning laser ophthalmoscopy study. *American Journal of Ophthalmology* 154: 174-86

Ooto S, Hangai M, Takayama K, Ueda-Arakawa N, Makiyama Y, et al. 2014. High-resolution imaging of photoreceptors in macular microholes. *Invest Ophthalmol.Vis.Sci.* 55: 5932-43

Ooto S, Hangai M, Takayama K, Ueda-Arakawa N, Tsujikawa A, et al. 2013. Comparison of cone pathologic changes in idiopathic macular telangiectasia types 1 and 2 using adaptive optics scanning laser ophthalmoscopy. *American Journal of Ophthalmology* 155: 1045-57

Ooto S, Hangai M, Yoshimura N. 2011c. Photoreceptor restoration in unilateral acute idiopathic maculopathy on adaptive optics scanning laser ophthalmoscopy. *Archives of Ophthalmology* 129: 1633-35

Pang CE, Suqin Y, Sherman J, Freund KB. 2015. New insights into stargardt disease with multimodal imaging. *Ophthalmic surgery, lasers & imaging retina* 46: 257-61

Paques M, Miloudi C, Kulcsar C, Leseigneur A, Chaumette C, Koch E. 2015. High-resolution imaging of gunn's dots. *Retina* 35: 120-4

Park SP, Hong IH, Tsang SH, Lee W, Horowitz J, et al. 2013. Disruption of the human cone photoreceptor mosaic from a defect in NR2E3 transcription factor function in young adults. *Graefes Arch.Clin.Exp.Ophthalmol.* 251: 2299-309

Park SP, Lee W, Bae EJ, Greenstein V, Sin BH, et al. 2014. Early Structural Anomalies Observed by High-Resolution Imaging in Two Related Cases of Autosomal-Dominant Retinitis Pigmentosa. *Ophthalmic Surg.Lasers Imaging Retina*: 1-5

Pinhas A, Razeen M, Dubow M, Gan A, Chui TY, et al. 2014. Assessment of perfused foveal microvascular density and identification of nonperfused capillaries in healthy and vasculopathic eyes. *Invest Ophthalmol Vis Sci* 55: 8056-66

Pyo PS, Hwan HI, Tsang SH, Chang S. 2013. Cellular imaging demonstrates genetic mosaicism in heterozygous carriers of an X-linked ciliopathy gene. *Eur.J.Hum.Genet.* 21: 1240-48

Querques G, Kamami-Levy C, Blanco-Garavito R, Georges A, Pedinielli A, et al. 2014. Appearance of medium-large drusen and reticular pseudodrusen on adaptive optics in age-related macular degeneration. *British Journal of Ophthalmology* 98: 1522-27

Querques G, Massamba N, Guigui B, Lea Q, Lamory B, et al. 2012. In vivo evaluation of photoreceptor mosaic in early onset large colloid drusen using adaptive optics. *Acta Ophthalmol.* 90: e327-e28

Ratnam K, Vastinsalo H, Roorda A, Sankila EM, Duncan JL. 2013. Cone structure in patients with usher syndrome type III and mutations in the Clarin 1 gene. *JAMA Ophthalmol.* 131: 67-74

Rha J, Dubis AM, Wagner-Schuman M, Tait DM, Godara P, et al. 2010. Spectral domain optical coherence tomography and adaptive optics: imaging photoreceptor layer morphology to interpret preclinical phenotypes. *Adv.Exp.Med.Biol.* 664: 309-16

Roorda A, Garcia CA, Martin JA, Poonja S, Queener H, et al. 2006. What can adaptive optics do for a scanning laser ophthalmoscope ? *Bull.Soc.Belge Ophtalmol.*: 231-44

Rossi EA, Achtman RL, Guidon A, Williams DR, Roorda A, et al. 2013a. Visual function and cortical organization in carriers of blue cone monochromacy. *PLoS One* 8: e57956

Rossi EA, Rangel-Fonseca P, Parkins K, Fischer W, Latchney LR, et al. 2013b. In vivo imaging of retinal pigment epithelium cells in age related macular degeneration. *Biomed.Opt.Express* 4: 2527-39

Saleh M, Debellemaniere G, Meillat M, Tumahai P, Bidaut GM, et al. 2014. Quantification of cone loss after surgery for retinal detachment involving the macula using adaptive optics. *British Journal of Ophthalmology* 98: 1343-48

Scoles D, Higgins BP, Cooper RF, Dubis AM, Summerfelt P, et al. 2014a. Microscopic inner retinal hyper-reflective phenotypes in retinal and neurologic disease. *Invest Ophthalmol.Vis.Sci.* 55: 4015-29

Scoles D, Sulai YN, Langlo CS, Fishman GA, Curcio CA, et al. 2014b. In vivo imaging of human cone photoreceptor inner segments. *Invest Ophthalmol.Vis.Sci.* 55: 4244-51

Song H, Latchney L, Williams D, Chung M. 2014. Fluorescence adaptive optics scanning laser ophthalmoscope for detection of reduced cones and hypoautofluorescent spots in fundus albipunctatus. *JAMA Ophthalmol.* 132: 1099-104

Sredar N, Ivers KM, Queener HM, Zouridakis G, Porter J. 2013. 3D modeling to characterize lamina cribrosa surface and pore geometries using in vivo images from normal and glaucomatous eyes. *Biomed.Opt.Express* 4: 1153-65

Stepien KE, Han DP, Schell J, Godara P, Rha J, Carroll J. 2009. Spectral-domain optical coherence tomography and adaptive optics may detect hydroxychloroquine retinal toxicity before symptomatic vision loss. *Trans.Am.Ophthalmol.Soc.* 107: 28-33

Stepien KE, Martinez WM, Dubis AM, Cooper RF, Dubra A, Carroll J. 2012. Subclinical photoreceptor disruption in response to severe head trauma. *Archives of Ophthalmology* 130: 400-02

Stepushina OA, Bol'shunov AV. 2011. [Combination of measurement of retinal vascular caliber, adaptive optics and fluorescent angiography in early diagnosis and monitoring of diabetic and hypertensive retinopathy]. *Vestn.Oftalmol.* 127: 29-31

Sundaram V, Wilde C, Aboshiha J, Cowing J, Han C, et al. 2014. Retinal structure and function in achromatopsia: implications for gene therapy. *Ophthalmology* 121: 234-45

Syed R, Sundquist SM, Ratnam K, Zayit-Soudry S, Zhang Y, et al. 2013. High-resolution images of retinal structure in patients with choroideremia. *Invest Ophthalmol.Vis.Sci.* 54: 950-61

Takayama K, Ooto S, Hangai M, Arakawa N, Oshima S, et al. 2012. High-resolution imaging of the retinal nerve fiber layer in normal eyes using adaptive optics scanning laser ophthalmoscopy. *PLoS One* 7: e33158

Tam J, Dhamdhere KP, Tiruveedhula P, Lujan BJ, Johnson RN, et al. 2012. Subclinical capillary changes in non-proliferative diabetic retinopathy. *Optometry and Vision Science* 89: E692-E703

Tam J, Dhamdhere KP, Tiruveedhula P, Manzanera S, Barez S, et al. 2011. Disruption of the retinal parafoveal capillary network in type 2 diabetes before the onset of diabetic retinopathy. *Invest Ophthalmol Vis Sci* 52: 9257-66

Telander DG, Choi SS, Zawadzki RJ, Berger N, Keltner JL, Werner JS. 2010. Microstructural Abnormalities Revealed by High Resolution Imaging Systems in Central Macular Arteriovenous Malformation. *Ophthalmic Surg.Lasers Imaging*: 1-4

Tojo N, Nakamura T, Ozaki H, Oka M, Oiwake T, Hayashi A. 2013. Analysis of macular cone photoreceptors in a case of occult macular dystrophy. *Clin.Ophthalmol.* 7: 859-64

Vincent A, Wright T, Garcia-Sanchez Y, Kisilak M, Campbell M, et al. 2013a. Phenotypic characteristics including in vivo cone photoreceptor mosaic in KCNV2-related "cone dystrophy with supernormal rod electroretinogram". *Invest Ophthalmol.Vis.Sci.* 54: 898-908

Vincent AL, Carroll J, Fishman GA, Sauer A, Sharp D, et al. 2013b. F45L Allele Does Not Cause Autosomal Dominant Retinitis Pigmentosa in a Large Caucasian Family. *Transl.Vis.Sci.Technol.* 2: 4

Wagner-Schuman M, Neitz J, Rha J, Williams DR, Neitz M, Carroll J. 2010. Color-deficient cone mosaics associated with Xq28 opsin mutations: a stop codon versus gene deletions. *Vision Research* 50: 2396-402

Wang Q, Tuten WS, Lujan BJ, Holland J, Bernstein PS, et al. 2015. Adaptive Optics Microperimetry and OCT Images Show Preserved Function and Recovery of Cone Visibility in Macular Telangiectasia Type 2 Retinal Lesions. *Invest Ophthalmol Vis Sci* 56: 778-86

Werner JS, Keltner JL, Zawadzki RJ, Choi SS. 2011. Outer retinal abnormalities associated with inner retinal pathology in nonglaucomatous and glaucomatous optic neuropathies. *Eye (Lond)* 25: 279-89

Wilk MA, McAllister JT, Cooper RF, Dubis AM, Patitucci TN, et al. 2014. Relationship between foveal cone specialization and pit morphology in albinism. *Invest Ophthalmol.Vis.Sci.* 55: 4186-98

Wolfing JI, Chung M, Carroll J, Roorda A, Williams DR. 2006. High-Resolution Retinal Imaging of Cone-Rod Dystrophy. *Ophthalmology* 113: 1014-19

Xue B, Choi SS, Doble N, Werner JS. 2007. Photoreceptor counting and montaging of en-face retinal images from an adaptive optics fundus camera. *J.Opt.Soc.Am.A Opt.Image Sci.Vis.* 24: 1364-72

Yokota S, Ooto S, Hangai M, Takayama K, Ueda-Arakawa N, et al. 2013. Objective assessment of foveal cone loss ratio in surgically closed macular holes using adaptive optics scanning laser ophthalmoscopy. *PLoS One* 8: e63786

Yoon MK, Roorda A, Zhang Y, Nakanishi C, Wong LJ, et al. 2009. Adaptive optics scanning laser ophthalmoscopy images in a family with the mitochondrial DNA T8993C mutation. *Invest Ophthalmol.Vis.Sci.* 50: 1838-47

Zayit-Soudry S, Duncan JL, Syed R, Menghini M, Roorda AJ. 2013. Cone structure imaged with adaptive optics scanning laser ophthalmoscopy in eyes with nonneovascular age-related macular degeneration. *Invest Ophthalmol.Vis.Sci.* 54: 7498-509

Zhang Y, Wang X, Rivero EB, Clark ME, Witherspoon CD, et al. 2014. Photoreceptor perturbation around subretinal drusenoid deposits as revealed by adaptive optics scanning laser ophthalmoscopy. *American Journal of Ophthalmology* 158: 584-96